CHAPTER 1

Optical Techniques in Transport Phenomena

C. V. HERMAN
Lehrstuhl A für Thermodynamik
TU München, Arcisstrasse 21
8000 München 2, Germany

D. MEWES
Institut für Verfahrenstechnik
Universität Hannover
Callinstrasse 36, 3000 Hannover 1, Germany

F. MAYINGER
Lehrstuhl A für Thermodynamik
TU München, Arcisstrasse 21
8000 München 2, Germany

1. INTRODUCTION

Optical measurement techniques use light as information carrier in order to obtain qualitative and quantitative data on the investigated phenomenon. The earliest applications of optical methods enabled visualization of physical processes in fluids (for example bubble flow in two phase flow, visualization of streamlines by adding dye into the liquid, flow visualization by smoke ...), some of them also providing quantitative data, but still they prevalently served to gain overall insight into the process and as introduction into further experimental research. Nowadays, optical techniques enable precise quantitative measurement of fluid parameters, like velocity, density, temperature, concentration, etc. The aim of the paper is to overview modern optical measuring techniques and to provide the reader with information necessary to reduce the choice for selection of optical methods, suitable for a specific application area.

The term optical methods is used in a broad sense in this paper, meaning techniques exploiting optical effects, like light absorption, reflection, scattering, etc. Optical measuring techniques belong to the family of nonintrusive

methods (except for optical fibre probes), together with other methods using waves of different character (sound waves, γ-rays, X-rays ...). Their main advantage is that they do not affect the process under investigation: the information is impressed into the light beam by the fluid. One essential requirement in the use of optical methods is to have a transparent fluid in order to transilluminate the investigated volume; the energy absorbed in the measurement volume from the probing light beam must be negligibly small to avoid influencing the process. The information impressed into the light waves by the phenomenon to be analysed is then detected by suitable means (photographic material, electronic sensors).

Further advantages of optical methods are the possibilities to achieve high spatial and temporal resolutions. Some of the methods are characterized by extremely high information density (like holography or speckle methods), where information on the complete parameter field can be reconstructed practically continuously. Optical methods enable the analysis of ultra-high-speed phenomena (for example real time interferometry), the temporal resolution is in such cases limited by the sensitivity of the photographic material, mechanical limitations of film transport, sensor inertia, etc.

The diverse optical methods are discussed both from the theoretical and the practical point of view, application examples are presented as far as the frame of the paper allows. In the references, the interested reader can find motivation and material for further reading.

2. CLASSIFICATION OF OPTICAL METHODS

In order to provide the reader of this article with general information on the optical techniques applied in the measurement of transport phenomena, the optical methods discussed in this paper and the process parameters to be measured are systematically presented in table 1. Thus, a general picture of the complexity of the subject can be gained, topics of special interest localized and, by using the table, chapters treating specific problems can easily be found. The categorization is motivated by practical requirements (to provide guidelines for experimental application), and it is not an attempt of a complete systematization — the field being much too complex for a unique presentation. The interested reader will find more general information and different viewpoints in the overview literature treating specific topics.

The optical methods treated in this paper are classified into two global groups. *Field measurements* (also termed image forming methods) provide the experimetator with information on the whole fluid field under investigation at a given moment. The information to be gained is spatially continuous and temporally discontinuous, the process can be observed, photographed or registered by a video camera or a high speed camera. Temporal data on instationary processes is thus obtained by taking a sequence of field measurements in the time interval of interest. The images recorded in the observation plane are two dimensional, and the information on the flow situation is integrated along the third spatial coordinate (for details see interferometric methods). *Local measurements* yield temporally continuous, spatially discon-

Transport process		Measurement method & physical effect	Field measurements									Local measurements			
			Natural methods	Addition of foreign materials	Holography	Methods based on refraktive index variation: Shadowgr.	Schlieren	Interference	Streaming birefringence	Speckle methods	Light scattering: Laser ind. luminesc.	LDA	linear Raman s.	CARS	Optical fibre probes
Single phase flow	Momentum transfer	density				R 3.4.2	R 3.4.3	R 3.4.4			R 5.1.2		R 5.1.3	R 5.1.4	
		velocity	T 3.1	T 3.2	R 3.3				R 3.5	R 3.6	R 5.1.2	T 5.1.1			
		stress		R 3.2								R 5.1.1			
	Heat transfer	temperature		T 3.2		R 3.4.2	R 3.4.3	R 3.4.4		R 3.6	R 5.1.2		R 5.1.3	R 5.1.4	
	Mass transfer	concentration		T 3.2		R 3.4.2	R 3.4.3	R 3.4.4			R 5.1.2		R 5.1.3	R 5.1.4	
	Heat & Mass transfer	Conc. & temp. field						R 3.4.4					R 5.1.3	R 5.1.4	
Multiphase flow	Particle -gas flow	particle velocities	T 3.1		R 3.3					R 3.6		R 5.1.1			
		particle concent.										R 5.1.1			
		particle diameter	T 3.1		R 3.3							R 5.1.1			
	Particle -liquid flow	particle velocities										R 5.1.1			
		particle concent.										R 5.1.1			
		particle diameter										R 5.1.1			
	Gas -liquid flow	droplet velocities	T 3.1		R 3.3					R 3.6		R 5.1.1			
		droplet diameter	T 3.1		R 3.3										T 5.2
		void fraction													T 5.2
		temperature						R 3.4.4							

TABLE 1. Overview of the optical methods treated in this publication and the physical processes to be measured (T - reported technical, engineering application, R - research and chapter in which the method is discussed).

tinuous data in a single point of the investigated volume: in order to obtain information on the investigated field, the measurement volume can sequentially be scanned. The optical information is registered by electro-optical detectors. In this paper, field measurements and their applications are treated in detail, and principles of local measurement techniques are presented.

The discussed measurement techniques are listed in table 1, partly according to the physical effects exploited in the measurement. A systematical presentation in this sense is a difficult task — due to the complexity of the optical effects involved — and the reader should consult specialized literature for further information. It has been attempted to correlate the optical measurement techniques and the physical phenomena investigated, by indicating reported applications in the table. **T** refers to possible technical (industrial) applications and **R** predominantly to reported applications in experimental research carried out in specialized laboratories. As the field is constantly developing, with new applications reported daily, this division is meant mainly as orientation. Parallel to the application type, the chapter in which the method is discussed is also referred in the table under the letters T or R.

The engineer/researcher faced with the problem of choosing the measurement method for the physical phenomenon he is investigating, has to carefully evaluate the problem itself (research or industrial measurement, parameters to be measured, accuracy, stationary or instationary phenomenon, dimensionality of the problem, local information or field measurements ...) and the optical techniques available and suitable for such measurements. In the paper, one chapter is devoted to tomographic measurements, which enable the reconstruction of three dimensional data from two dimensional field information. Manual evaluation of flow visualization images is a tedious procedure, made easier by modern image processing techniques discussed in chapter 6. The experimental and computational effort and the pragmatical aspects, like the cost of the instrumentation needed to realize a certain measurement, must be taken into account in order to come to an optimal choice.

3. FIELD MEASUREMENTS

3.1 NATURAL METHODS OF FLOW VISUALIZATION

Numerous natural phenomena are visualized without the need to add foreign materials into the flow in course of the experimental investigation. These processes are characterized by natural presence of foreign additives, by existence of the gas-liquid interface in two phase flow, or other effects providing sufficient contrast for the flow pattern to become visible. The phenomena can thus be observed, photographed or filmed, in order to provide permanent records, from which a qualitative picture of the process and quantitative data (in a temporal sequence in instationary flows) is obtained.

Common examples of natural flow visualization are smoke from a chimney, surface waves on the sea, vortex flow in a river, cloud formations ... Phenomena in high-speed jets can be recorded by high speed cinematography, photographs of two-phase flow phenomena, like bubble flow or boiling, are

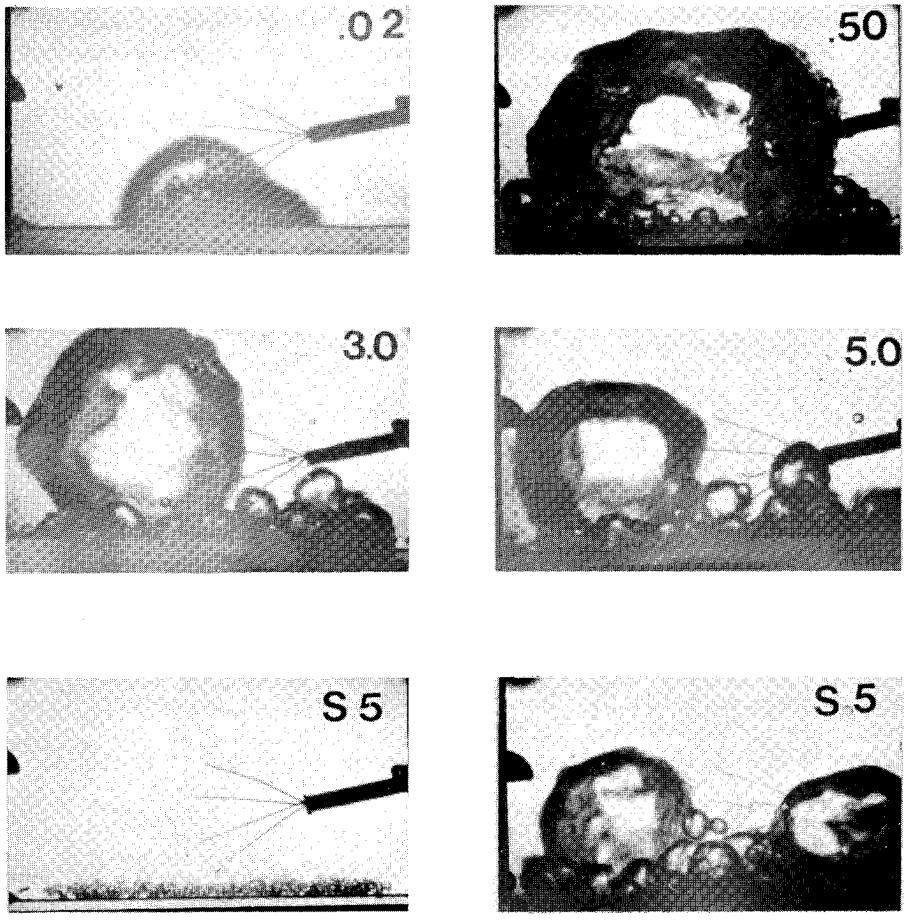

FIGURE 1. Natural flow visualization of boiling phenomena. The difference between boiling under microgravity and conventional boiling is recognized in the lack of heat transfer mechanisms due to buoyancy effects (for example transport of latent energy through bubble break-off, drift flow). Solely mechanisms independent from buoyancy, like condensation or evaporation, are responsible for the energy transport. The first four pictures illustrate the generation of the first bubble under microgravity in subcooled boiling of R113 ($T_\infty = 30°C$, $T_{sat} = 47°C$, $p = 1\ bar$) 0.02, 0.5, 3.0 and 5.0 seconds after the onset of the boiling process. After a short period (approximately 1s) the big first bubble (the dimensions of the picture frame are 40 mm · 25 mm) condenses, and stationary boiling conditions start to develop. The comparison of stationary boiling conditions(S5, $\dot{q} = 5\ W/cm^2$) shows drastic changes in bubble size. In spite of this, heat transfer coefficients under microgravity are only insignificantly smaller than under terrestial conditions (photographs by Zell, Straub and Vogel, for more details see Zell and Straub (1985)).

well known in the literature. Interesting visualization examples of such processes can be found in Van Dyke (1982), Visualized Flow (1988), Gad-el-Hak (1988), and others.

3.2 FLOW VISUALIZATION BY ADDITION OF FOREIGN MATERIALS

In order to gain an overall picture of a complex flow situation, knowledge of velocity vectors, pathlines (particle paths — trajectories of a particular fluid particle in the flow field as a function of time), streamlines (curves tangential to the instantaneous direction of the flow velocity in all points of the flow field) and streaklines (instantaneous locus of the fluid particles which have passed through a particular point in the flow) is essential. As most liquids and gases are transparent, in order to visually observe, record or measure the characteristic parameters of fluid motion, foreign materials (additives, tracers) are introduced into the fluid under specific conditions. It is assumed that the motion of the particles is identical to that of the fluid (particles should be small enough with densities corresponding to the denstity of the fluid), and in the experiments, the motion of foreign particles is observed.

Liquids can be marked by dyes (by injecting a dye or by initiating a chemical reaction causing color change); in gas flows, smoke generation by various techniques is commonly used. Velocity measurements in liquids and gases can be realized by evaluation of images obtained by particle tracking, the choice of particle size and material being strongly dependent on the specific application. Velocity profiles in water can be visualized by electrochemical methods, the hydrogen bubble technique or by using photocromatic and luminescent dyes.

By the addition of foreign materials, fluid flow on the surface of a solid body can be visualized, and, in certain cases, quantitative information is provided in this way. By means of the oil film technique (the solid surface is coated with oil containing pigment particles), information on the direction of the flow, on the location of the transition from laminar to turbulent flow, as well as locations of flow separation and reattachment are observable. Also, skin friction measurement using the oil film technique has been reported in the literature. Similarly, by coating solid surfaces with appropriate materials, mass transfer from a surface can be visualized.

The use of thermocromatic dyes provides a means for heat transfer visualization. Temperature sensitive paints react with color change to changes of temperature, thus providing patterns in which a specific color corresponds to a curve of constant temperature. Apart from surface temperatures, temperatures and velocities in a heated volume can be visualized using suitable tracers.

The techniques applied in flow visualization by addition of foreign materials are numerous and widely used, in order to support the experimentator with valuable information on flow behaviour. Tracer materials, experimental techniques, illumination problems and finally the interpretation of results,

are complex problems, strongly dependent on the specific physical problem under investigation. The publications available in this field are very comprehensive, and the reader is referred to the overview literature for further information and details (Werle (1973), Mueller(1980), Van Dyke (1982), Merzkirch (1987), Visualized Flow (1988), Gad-el-Hak (1988) and the Proceedings of the International Symposia on Flow Visualization, Tokyo 1977, Bochum 1980, Ann Arbor 1983, Paris 1986 and Prague 1989).

3.3 HOLOGRAPHY

3.3.1 Principles of holography

Holography is a two-step procedure for recording and reconstructing coherent light waves. The light wave to be reconstructed is called the object wave. The reconstruction of the object wave requires the reproduction of the complex amplitude of the wave at one plane in space. As conventional detectors and photographic film respond to irradiance and enable the recording of the amplitude, it was necessary to convert the phase distribution into an irradiance pattern. This is possible by using the optical recording technique, holography, invented by Gabor in 1949. The general theory of holography is very comprehensive and the reader is referred to the literature for further information (Gabor (1948), Gabor (1949), Collier, Burckhardt, Lin (1971), Vest (1979), Ostrovsky, Butusov, Ostrovskaya (1980), Jones and Wykes (1983), Hariharan (1984), Ostrowski (1988) and others). Holography has numerous application areas in different technical disciplines, and in this paper only the elements of the holographic technique relevant for measurements in transport processes will be considered.

The technique of *in-line holography* (described by Gabor (1948) and Gabor (1949)) was used extensively for forming three dimensional images of aerosols, sprays and distributions of small particles. In this work, *off-axis holography*, commonly used in interferometry and other applications, will be discussed in more detail. The principles of the holographic recording and reconstruction are illustrated in figure 2. The object to be recorded is illuminated by monochromatic light and the light wave reflected from the object, the object wave, falls directly onto a photographic plate. This wave is completely described by the amplitude and phase distribution of the light waves emanating from the object. The goal is to record these distributions in order to enable their reconstruction later. The recording of the amplitude presents no problem, as it has already been explained. In order to record the phase of the object wave, the effect of interference is used, and the phase distribution is converted into irradiance distribution. In order to achieve this, a reference wave is superimposed to the object wave. If coherent light is used, an interference pattern is generated. The photographic plate illuminated in this way is called the hologram after the development and it contains complete information on the object wave. The phase distribution is recorded in the interference pattern and the amplitude in form of varying contrast. When illuminating the hologram by the original reference beam only, it will function as a diffraction grating with spatially varying diffraction constant.

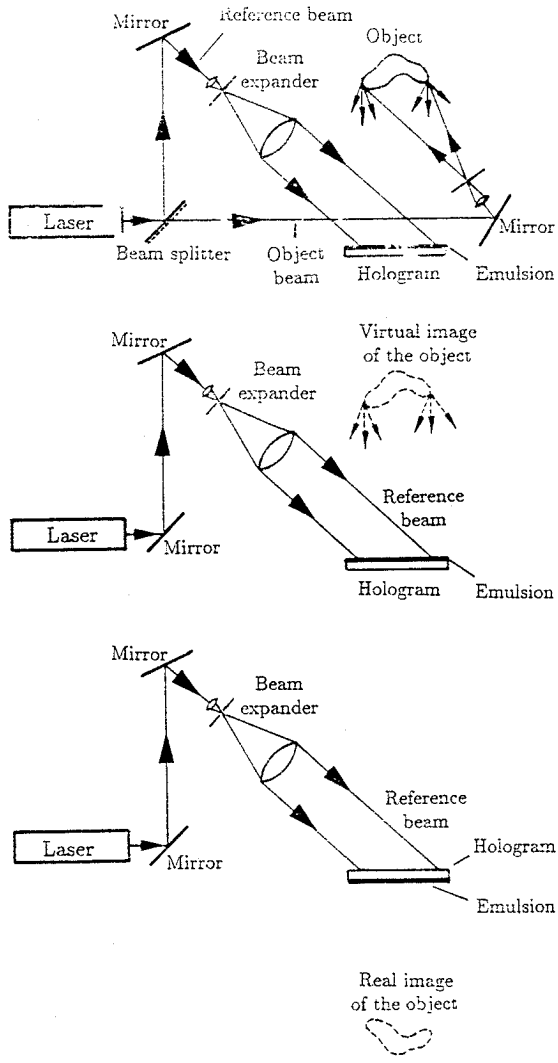

FIGURE 2. Schematic of the optical setup for off-axis holography: (a) recording a hologram, (b) reconstructing the virtual image, (c) reconstructing the real image (Vest (1979)).

In this way, both a real image and a virtual image can be reconstructed as shown in figure 2.

3.3.2 Pulsed laser holography in the study of high speed phenomena

One application of holography in the study of transport phenomena, the *characterization of sprays*, will be explained here in detail. Pulsed-laser holography has been used in the measurement of size and velocity distribution of spray droplets for characterization of sprays by Chavez and Mayinger (1988). The *optical setup* for holographic recording is presented in figure 3a. A pulsed ruby laser capable of operating in single-pulse mode (energy output $1J$, pulse width $30ns$) and double-pulse mode (pulses of $0.5J$ at intervals of 1 to $800\mu s$) is used as a light source. The collimated object beam is led into

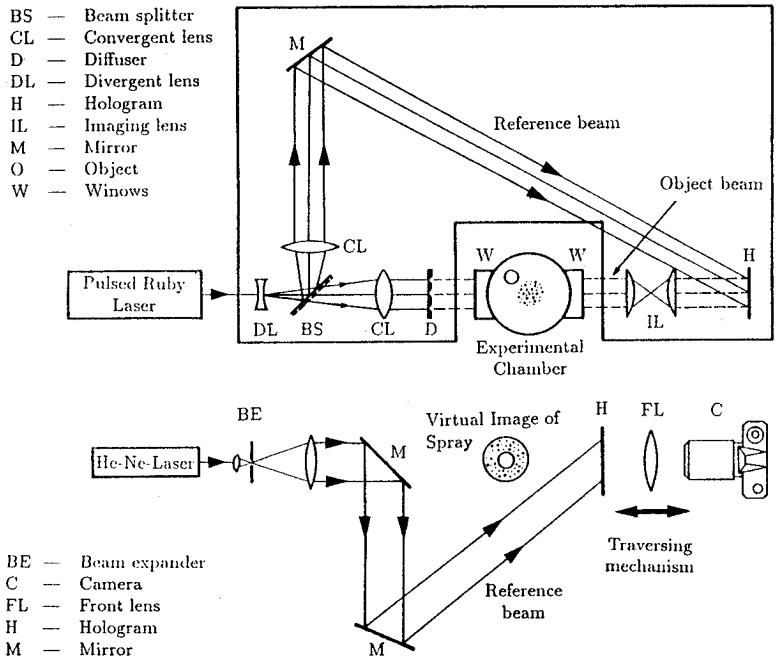

FIGURE 3. Schematic of the optical setup for pulsed laser holography: (a) recording and (b) reconstruction of holograms (Chavez and Mayinger (1988)).

the experimental chamber through a diffuser (providing uniform illumination of the object) and is transmitted through the spray. The imaging lenses were placed between the spray and the holographic plate to produce a conjugate image of the spray close to the holographic plate. In the reconstruction, a He-Ne laser beam was used to replace the reference beam and illuminate the hologram, as presented in figure 3b. This arrangement enables the photographing of the virtual image of the reconstructed hologram. The holographic image is then analysed by varying the focusing length of the front

lens and thus sweeping the full length of the image. In this way, three dimensional information was converted into a set of two dimensional images.

In the *experiments*, a hollow cone type swirl nozzle of $0.7mm$ in bore diameter was used; in one case water was injected into atmosphere air, and in the second situation subcooled refrigerant R113 was injected into its own saturated vapour. Photographs of two single-pulsed holograms are presented in figure 4. Holograms were evaluated both manually and by image processing (to be discussed in chapter 6). *Single-pulsed holograms* enable observation of the form of the spray and measurement of droplet size, break-up length and spray angle. From *double pulsed holograms* droplet velocities can be evaluated. Such measurements are important complements to speckle methods or to time resolved measurements, like phase-Doppler anemometry.

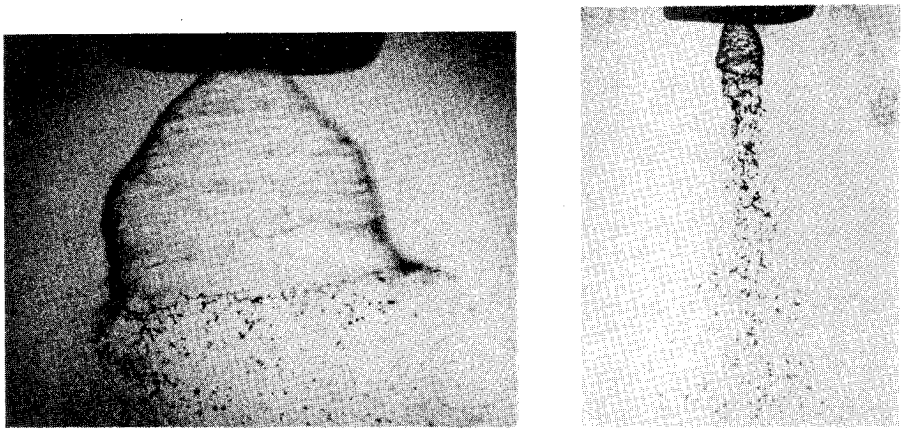

FIGURE 4. Typical photographs of reconstructed single-pulsed holograms: (a) water spray in atmospheric air ($\dot{m} = 116g/min$, temperature of water $T = 16°C$) and (b) R113 spray in its own saturated vapour ($\dot{m} = 64.5$ g/min, temperature of liquid $T_L = 25°C$, temperature of vapour $T_v = 47°C$, vapour pressure $p_v = 0.1MPa$), (Chavez and Mayinger (1988)).

3.3.3 Other applications

The holographic recording technique is extensively used in flow measurements. In single phase flow, it provides means to freeze the three dimensional picture of the flow. It can be combined with tracer methods, and, in this way, in the reconstructed image the position of the individual tracer particles can be analysed. If the double-pulse technique is used, flow velocities can be evaluated by determining the vector change in tracer position. Also, three dimensional spatial positions and velocity fields of a particle can be obtained by measuring the radii of concentric interference fringes of the diffractive image of a single spherical particle. Different optical visualization systems can be combined with holography, in order to eliminate the temporal limitations to perform the experiments in the analysis of high speed

phenomena. The combination of holography with schlieren and shadowgraph techniques is used in flow visualization studies. One important and frequent application of this recording method, holographic interferometry, will be discussed in detail in the following chapter. The reader can find details on the application of holography in flow visualization in the review literature (Lauterborn and Vogel (1984), Gad-el-Hak (1988), Merzkirch (1987)).

In two phase flow, holography can be used instead of photography to determine aerosol, droplet and particle size and velocity. These applications were reviewed by Hewitt (1978) and Mayinger (1987).

3.4 METHODS BASED ON THE REFRACTIVE INDEX VARIATION

3.4.1 Introduction

In this chapter, optical methods based on the refractive index variation, belonging to the class of image forming methods, will be discussed. The refractive index n is a physical property of the fluid, and it depends on the density of the fluid ρ and the wavelength of light λ. The relation between the density of the fluid and the refractive index is given by the Lorentz-Lorenz equation

$$N(\lambda) = \frac{n(\lambda)^2 - 1}{n(\lambda)^2 + 2} \frac{M}{\rho}, \tag{3.4.1}$$

where $N(\lambda)$ is the molecular refractivity (function of the substance and the wavelength of light) and M is the molecular mass. The simplified form of the Lorentz-Lorenz equation is the Gladstone-Dale equation, valid for gases for which the value of the refractive index is close to 1.

$$N(\lambda) = \frac{2}{3} (n(\lambda) - 1) \frac{M}{\rho} \tag{3.4.2}$$

A wide variety of phenomena exists which can be analysed by the aid of methods using the refractive index/density variation. The most frequent *application areas* are the analysis of convection heat transfer in gases and liquids, mass transfer, simultaneous heat and mass transfer, phenomena of mixing of two fluids of different densities, analysis of density changes in compressible flow (for example shock waves), combustion processes characterized by high temperature differences and mixing, plasma flows, etc. One essential requirement for the application of these techniques is to have a transparent fluid.

The basic principles of the method are illustrated in figure 5. The wavefront of the light beam entering the test section is known. This wavefront is distorted inside the test section, due to the inhomogenities of the refractive index field. The deformation of the light beam takes the form of *deflection* (the direction of propagation is changed) and *phase change*. The optical methods discussed in this chapter enable the determination of the distorted wavefront, and thus also the corresponding refractive index field, causing the

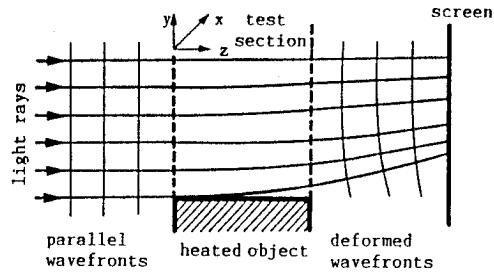

FIGURE 5. Deflection of light beams and distortion of plane wavefronts in the inhomogenous refractive index field — the two effects exploited in methods using the refractive index variation.

deformation. From the refractive index field, the density field, e.g. concentration, temperature etc. can be reconstructed through measurements. As the human eye is not capable of distinguishing variations in phase and direction of light, these variations have to be converted into changes of intensity by the different optical techniques.

As it is obvious from figure 5, the light beam is passing through the test section in the direction of the z axis, and is incapable of distinguishing refractive index variations in this direction. Thus, only two dimensional refractive index fields $n(x, y)$ and special cases of three dimensional fields $n(x, y, z)$ (like objects with axial symmetry) can be analysed in this way. In order to obtain three dimensional information, the test section must be viewed from several directions. The reconstruction of three dimensional fields through optical methods is called optical tomography, and will be discussed in detail in a separate chapter later in this paper.

An overview of the application of these methods in heat transfer was given by Hauf and Grigull (1970), in flow visualization by Merzkirch (1987), and in Van Dyke (1982) and Visualized Flow (1987), examples of visualized refractive index fields for a wide range of physical phenomena are given.

3.4.2 Shadowgraph methods

Shadowgraph methods belong to the simplest and oldest flow visualization methods using the effect of refractive index variation. Information on density variation in the test field is obtained from *light deflection.* The intensity contrast is proportional to changes of the second derivative of the refractive index. The basic optical setup used for these measurements is presented in figure 6. It consists of a point light source, a lens providing a bundle of parallel light rays — which are subject to deflection in the test section. This deflection causes light intensity variations to be observed on the screen. The method is frequently applied to the visualization of shock waves (Van Dyke (1982), Merzkirch (1987), Visualized Flow (1988)), it can be used in heat transfer measurements (Hauf and Grigull (1970)), and concentration measurements. Data obtained through shadowgraph methods is

less suitable for quantitative evaluation than data obtained through more sensitive methods, like the schlieren or the interferometric techniques.

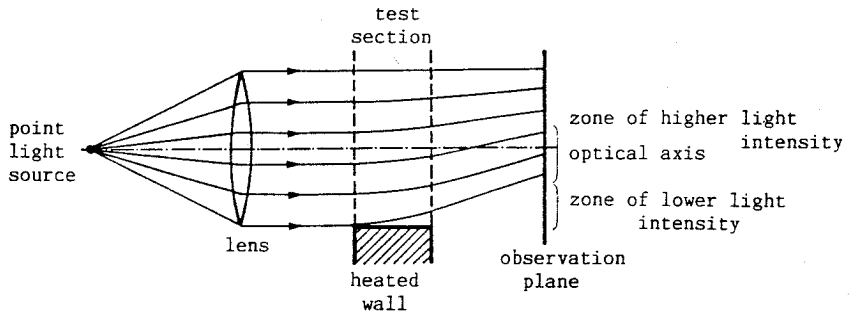

FIGURE 6. Schematic of the optical arrangement for the shadowgraph technique.

3.4.3 Schlieren methods

The simplest schlieren arrangement is obtained by modifying the shadowgraph setup through adding another lens after the test section, and a knife edge in the focal point of this lens. The *Toepler schlieren apparatus*, first described by Toepler in 1864, is presented schematically in figure 7.

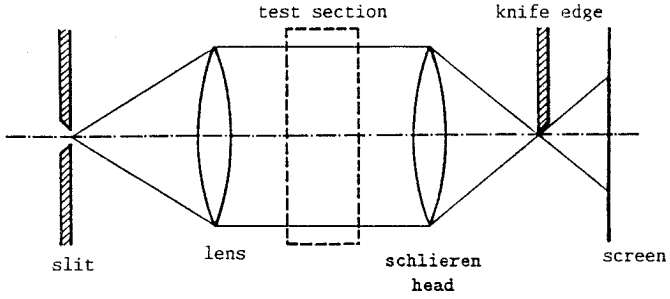

FIGURE 7. Schematic of the Toepler schlieren apparatus.

The light source in this setup is a vertical slit. Parallel rays, which pass the test section, are obtained after the first lens. The second lens, called schlieren head, images the central plane of the test section onto the observation plane. A knife edge, introduced at the focal plane of the second lens, parallel to the slit, covers one half of the light source slit, thus reducing the illumination of the screen. The deflected light rays cause a shift of the light source image, and, in this way, refractive index gradients normal to the knife edge can be measured. The relative change of light intensity is, in this situation, proportional to the first derivative of the refractive index. This setup is more sensitive to density changes than the shadowgraph, thus being more

suitable for quantitative evaluation. The evaluation technique of schlieren images has been described in detail in the work of Schardin (1934) and Hauf and Grigull (1970). The evaluation requires to quantitatively distinguish between shades of gray, which is not a very reliable method, so that schlieren techniques are recommended mainly for qualitative analyses of physical phenomena.

Many *modifications of schlieren techniques* have been described in the literature, and the interested reader is referred to the work of Schardin (1934), Hauf and Grigull (1970) and Merzkirch (1987). The purpose of the modifications introduced into the basic optical setup is the increase of the sensitivity of the method, in order to provide images more suitable for accurate quantitative measurements and also to reduce noise.

Very impressive schlieren images have been obtained by *color schlieren techniques,* where light deflection is converted into color. In these setups, the use of a white light source is essential. Different techniques are available to obtain the desired color contrast, color coding and resolution and to achieve sufficient sensitivity and measuring range of the schlieren technique. Thus, this method provides additional information for interpretation. Common application areas of the color schlieren techniques are compressible flow visualization, convective heat transfer, mixing and combustion. An extensive overview of the literature on this subject was given by Settles (1980) and Howes (1984).

3.4.4 Interference methods

Interference methods enable visualization of the information contained in the deformed wavefront (*phase change*) after passing through the phase object. These methods enable high accuracy measurements, and the obtained signal is proportional to the refractive index n. The interference pattern consists of lines of constant phase difference, and the original undeformed wave front serves as reference. In the special case of the infinite fringe field alignment, these lines represent isotherms.

In this paper, *reference beam interferometry* and its applications will be discussed in detail. The application of interferometers in the study of phase objects dates from the end of the 19th century. In the case of reference beam interferometers, the interference of two waves is visualized: one has passed through the test section and it is called the measuring beam, the one propagating outside of the test section is the reference beam. In the analysis of transport phenomena, the most commonly used interferometers are the Mach-Zehnder interferometer and the holographic interferometer. Also, well known constructions are the Jamin interferometer and the Michelson interferometer (for a more detailed description of these techniques the reader should consult the work of Hauf and Grigull (1970)). Two beam interferometers, where both beams pass the test section separated by a small distance, are called *shearing interferometers,* and are discussed in detail by Merzkirch (1987).

The Mach-Zehnder interferometer

The *basic optical setup* of the Mach-Zehnder interferometer is presented schematically in figure 8. In this setup, a bundle of parallel light beams of relatively large diameter is obtained by a point light source and a lens. The original beam is split into the reference beam and the measuring beam by a semitransparent mirror. The measuring beam traverses the test section, and is recombined with the reference beam by the second semitransparent mirror — to enable the interference of the two. The *infinite fringe field alignment* of this interferometer corresponds to the situation when all mirrors are inclined exactly the same angle to the parallel light beam. In this case, the wavefronts of the measuring and the reference beams coincide, and in the recording plane no fringes appear. The second basic alignment of the Mach-Zehnder interferometer is the *finite fringe field alignment*, to be achieved by tilting one of the mirrors by a small angle. In the recording plane, a regular fringe pattern appears. The technique of Mach-Zehnder interferometry has been discussed in detail by Hauf and Grigull (1970).

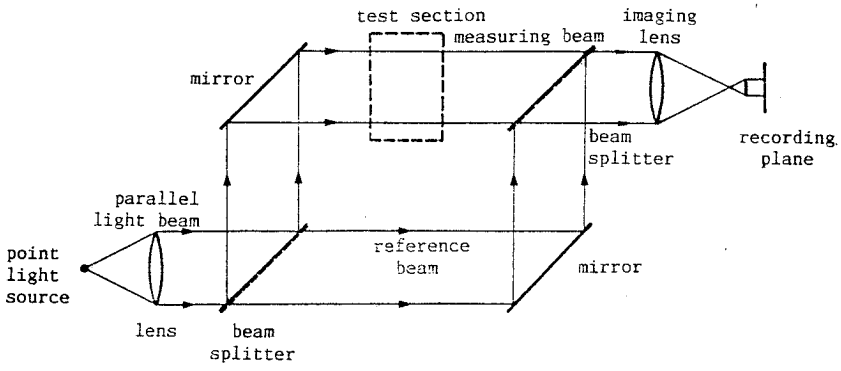

FIGURE 8. Schematic of the basic optical setup of the Mach-Zehnder interferometer.

The most frequent *applications* of the Mach-Zehnder interferometer are visualizations of density fields in compressible flows, measurements of temperature fields and concentration fields. In the *evaluation of interferograms*, the phase difference, visualized by light and dark fringes and expressed as a multiple of the wavelength of light λ, can be evaluated as the difference between the optical path of the measuring beam (index M) and the reference beam (index R)

$$S(x,y)\ \lambda = \int_0^l (n(x,y)_M\ -\ n(x,y)_R)\ dz. \qquad (3.4.3)$$

Intensity minima are obtained for

$$|\ S\ | = 1/2;\ 3/2;\ 5/2;\ \ldots \text{ (dark fringes)}$$

and intensity maxima for

$$| S | = 0;\ 1;\ 2;\ 3;\ \ldots \text{ (light fringes).}$$

If the refractive index for the reference beam $n(x,y)_R$ is known, the two dimensional refractive index field can be evaluated from the interferograms as follows

$$S(x,y)\ \lambda = l(n(x,y)_M\ -\ n_\infty) \quad \text{for} \quad n(x,y)_R = n_\infty = const. \tag{3.4.4}$$

If there is only one fluid in the test section and the pressure is kept constant, density variations are due only to changes in the temperature of the fluid. If the fluid is a gas, by combining the ideal gas equation of state and equation (3.4.2), the following form of the Gladstone-Dale equation is obtained

$$N(\lambda) = \frac{2RT}{3p}\ (n(\lambda)\ -\ 1). \tag{3.4.5}$$

In this equation, R is the universal gas constant ($R = 8.314 J/molK$) and p is the pressure. Thus, entering (3.4.5) into (3.4.4). the temperature corresponding to a certain fringe shift can be evaluated as

$$T(x,y) = \left[\frac{S(x,y)2\lambda R}{3N(\lambda)pl}\ +\ \frac{1}{T_\infty}\right]. \tag{3.4.6}$$

Local heat transfer coefficients α can easily be found by measuring temperature gradients at the wall $(dT/dy)_W$. The finite fringe field technique is well suited for such measurements, as the temperature gradient at the wall can be determined by measuring the slope of the fringes. In the case of the laminar thermal boundary layer the heat transfer coefficient is evaluated as

$$\alpha = \frac{-k\ (dT/dy)_W}{T_W\ -\ T_\infty}, \tag{3.4.7}$$

where k is the thermal conductivity, T_W the temperature of the wall and T_∞ the reference temperature.

The Mach-Zehnder interferometer is an instrument requiring high precision mechanical performance, high stability and high quality of both mechanical and optical components. The necessary optical and mechanical tolerances of the elements are in the order of one tenth of the wavelength of light. Thus, the instrument is very expensive, the costs of it increasing with the size of the field of view. The requirements concerning high quality and precision of the optical and mechanical components also apply to the test section windows; optical inhomogenities of the glass may introduce additional deformation of the wavefronts and thus reduce the quality of interferograms, or, in extreme cases, destroy them completely (Vest (1979), Merzkirch (1987)). These requirements certainly limit possible application areas of conventional interferometry. Before the discovery of coherent light sources (lasers) the

alignment of the Mach-Zehnder interferometer was very complicated, because of the extremely small coherence length of the commonly used mercury vapor lamps (0.03 - 0.2 mm). Using lasers (the coherence length of common He-Ne lasers is in the range of 20 cm), the alignment procedure ceased to be a serious problem. Nowadays, it is possible to overcome many of the difficulties presented by classical interferometry by introducing the holographic recording technique into interferometry.

Holographic interferometry

Holographic interferometry can be defined as an optical measurement technique based on the comparison of wavefronts, where at least one of the wavefronts is reconstructed holographically (Vest (1979)). The basic principles of holography have been presented in the preceeding chapter, and here only elements relevant for holographic interferometry will be discussed. For more details about the technique, the reader is referred to the very comprehensive literature on this topic (Collier et al. (1971), Panknin (1974), Vest (1979), Ostrovsky et al. (1980), Wernicke and Osten (1982), Jones and Wykes (1983) and others). The aim of this chapter is to present the basic principles of holographic interferometry, and discuss its applications in the study of transport phenomena.

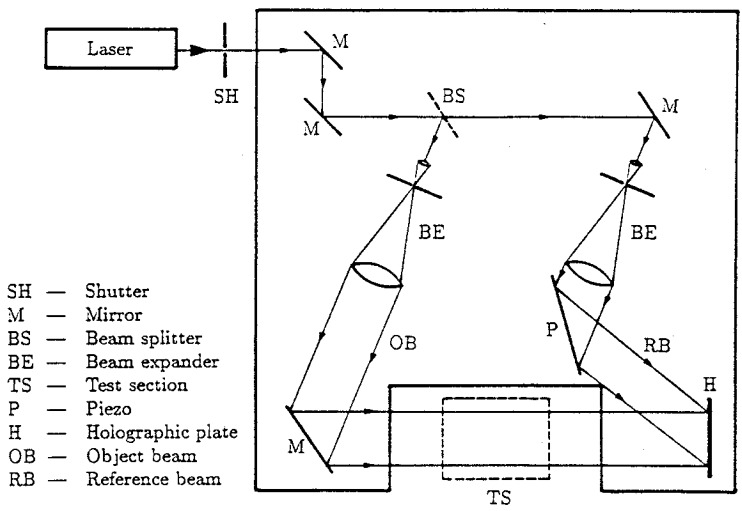

FIGURE 9. Schematic of the optical setup used in the double exposure and real time methods.

The method developed rapidly after the invention of the holographic recording technique (by Gabor (1949)) and the discovery of the laser. In the following years, new techniques and applications were reported, and very soon, holographic interferometry has become a generally accepted method in the analysis of transport phenomena, as it has been shown by Mayinger and

Panknin (1974). Holographic interferometry has numerous advantages over classical interferometry, and, in order to understand these advantages, one commonly used technique will be discussed first.

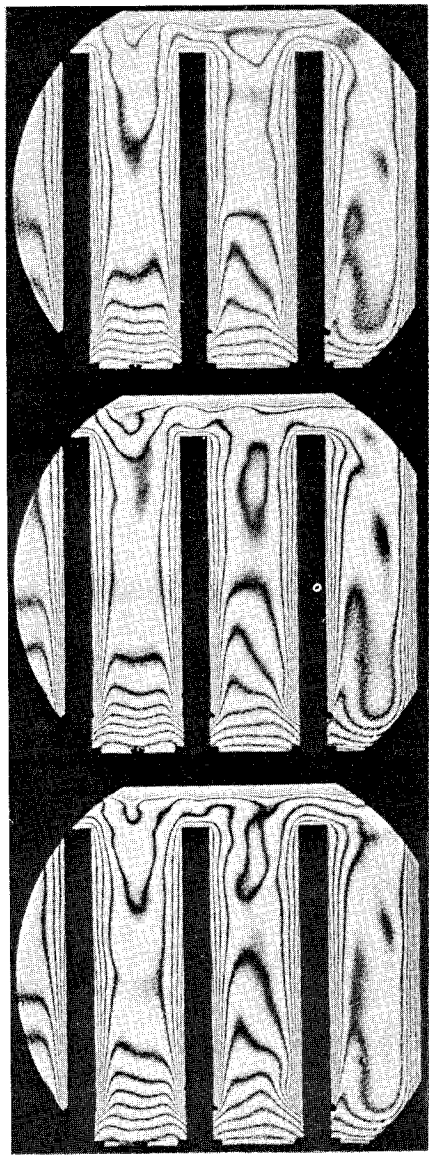

FIGURE 10. Holographic interferometry in the study of heat transfer in free convection. In the pictures, a series of three interferograms of free convection heat transfer in an enclosure, obtained by the real time method, is presented. The top and bottom surface of the rectangular enclosure is cooled to a temperature $T_C = 10\ ^\circ C$. The side walls (the right one is in the picture) are adiabatic, and inside the enclosure four plates (three of them in the picture) are kept on a temperature $T_H = 60\ ^\circ C$. The Rayleigh number for this situation is $Ra = 7.78\ 10^4$. The free convection process is instationary, and the photographs were taken at:
$t = t_0$
$t = t_0 + 0.5s$
$t = t_0 + 1s$,
respectively.
In the photographs, packages of cold air falling from top to bottom between the vertical plates can be observed (photograph, Z. Wang, Lehrstuhl A für Thermodynamik, TU München).

A standard *optical arrangement* which can be used both in the double exposure and in the real time methods, is presented in figure 9. The light source is a laser. The laser beam is divided into the reference beam and the

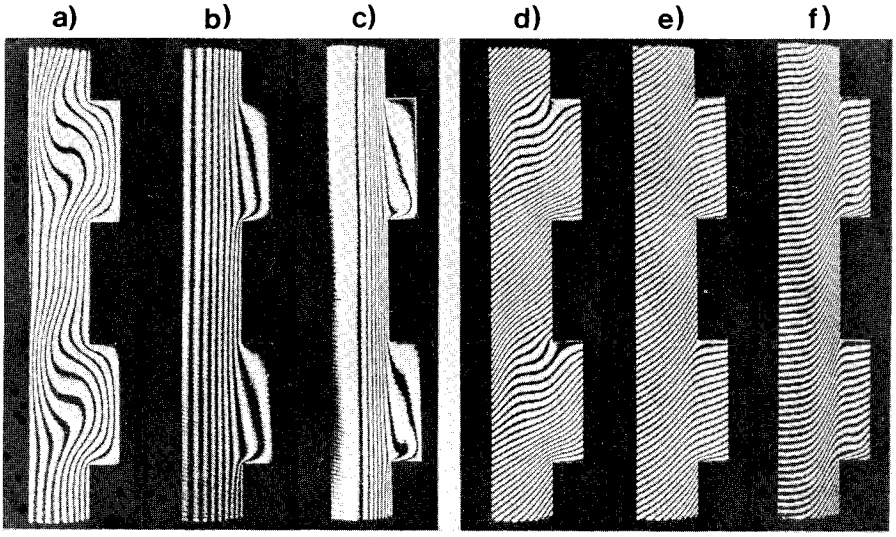

FIGURE 11. Holographic interferometry in the study of convection heat transfer. The figure illustrates temperature fields in free convection ((a) and (d)), and the development of the thermal boundary layer in laminar forced convection flow in a grooved channel. In the pictures, interferograms of the third and fourth groove are presented. In forced convection, the flow is fully developed hydrodynamically, the bulk fluid (air) temperature being $T_C = 23.2\ ^\circ C$. The grooved wall is heated ($T_H = 53.2\ ^\circ C$), and the temperature of the plain wall is T_C. The interferograms stand for free convection and Reynolds numbers $Re = 354$ ((b), (e)) and $Re = 1177$ ((c),(f)), respectively. In figures (a), (b), (c) the interferograms were obtained by the infinite fringe field adjustment, where stripes correspond to isotherms, and in figures (d), (e), (f) the same physical situation was photographed for the finite fringe field adjustment (Herman and Mayinger (1989)).

measuring beam (object beam) by means of a, usually variable, semitransparent mirror (beam splitter). The beams are then expanded into parallel light ray bundles by a telescope, which consists of a microscope objective, a spatial filter and a collimating lens. The object waves pass through the test section with the phase object (temperature field, concentration field etc.) and then fall onto the photographic plate. The reference beam falls directly onto the photographic plate. In the *double exposure technique,* several object waves can be recorded, one after the other, on the photographic plate. Usually, one of these waves corresponds to the undisturbed state of the phase object. The photographic plate is then developed and exactly repositioned into the plate holder. This developed photographic plate is called the hologram. By illuminating it with the reference wave, all recorded waves can be reconstructed.

If they differ slightly, an effect of macroscopic interference can be ob-

served, due to the difference in the object waves. The interferometric pattern is similar to the one obtained by the Mach-Zehnder interferometer. At this point, the *fundamental differences between the classical interferometric methods and holographic interferometry* can be discussed. The essential difference is, that in holographic interferometry the interfering waves are separated temporally (they pass through the test section at different moments) rather than spatially, as in the Mach-Zehnder interferometer, where the measuring beam and the reference beam travel different optical paths. The basic advantage of holographic interferometry , the cancellation of pathlength errors, is due to this effect: as both waves pass through the same object space, any noise due to imperfections of the test section windows, mirrors or lenses is eliminated. This means, that with relatively lower quality windows and optical components, it is possible to achieve interferograms of good quality. Thus, cheaper components can be used and the whole setup is easier to adjust, because the coherence length is not a critical issue any more. In holographic interferometry, permanent holographic records of the probing wavefront and the wavefronts to be compared are available.

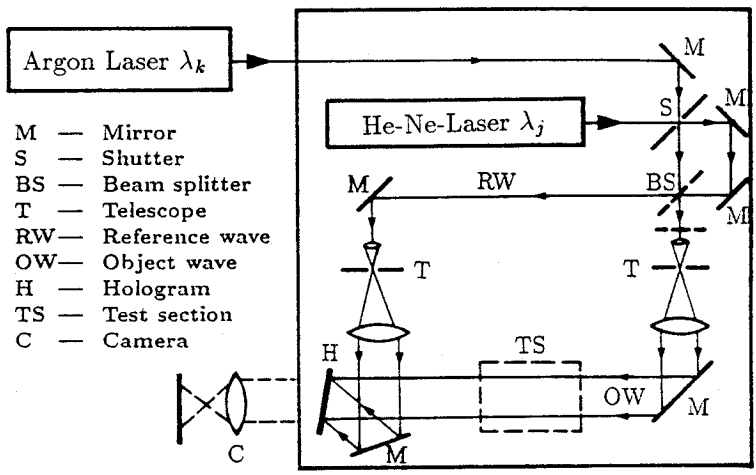

FIGURE 12. Optical arrangement for two wavelength holographic interferometry.

The results obtained by the double exposure technique discussed above, can, in most situations, be achieved by classical plane wave interferometric techniques (although holography offers significant advantages). One entirely new quality of holographic recording is the possibility to store three dimensional information on the phase object by *diffuse illumination interferometry.* In diffuse illumination interferometry, the object wave is scattered by a diffusing plate, placed into the expanded laser beam in front of the phase object. A single diffuse illumination holographic interferogram contains information obtainable from a large number of plane wave interferograms taken with different viewing directions. Such holograms can be observed from different

directions with the unaided eye. Additional advatages are the uniform average irradiance of the interferograms and the reduction of noise due to dust particles or small errors in the optical components.

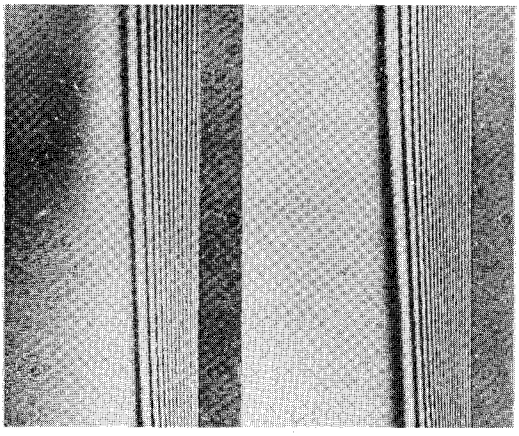

FIGURE 13. Simultaneous development of temperature and concentration boundary layers on a heated flat plate coated with naphtalene: interferograms obtained by He-Ne laser and argon laser.

Studies have shown that the *accuracy* achieved by holographic interferometry is identical to the accuracy of classical interferometric methods, although the fringe pattern shows a rougher structure mainly due to laser speckle effects. The holographic technique enables the analysis of ultra high speed phenomena using pulsed ruby lasers when taking the interferogram, and continuous He-Ne lasers in the reconstruction.

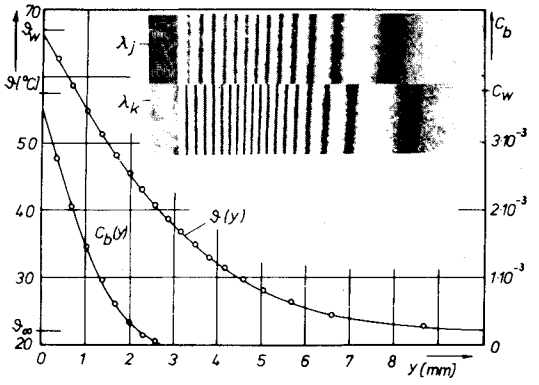

FIGURE 14. Interferograms of different wavelengths and the corresponding temperature and concentration profiles in a laminar boundary layer.

Holographic interferometry is also suitable to investigate transient phenomena and continuously observe the process by using the *real time method,* a single exposure technique. In the first exposure, the comparison wave is recorded, and the hologram developed, fixed and repositioned accurately into the plate holder. The comparison wave is reconstructed by illuminating the hologram with the reference wave. The reconstructed wave can now be superimposed to the momentary object wave. If the object wave corresponds to the original state in which the hologram was taken, no interference fringes appear (infinite fringe field adjustment). When the heat or mass transfer process is started, the resulting object wave is distorted, and behind the hologram, the object wave and the reference wave interfere and form an interference pattern which can be observed continuously and also filmed or photographed. This means, that the reference state has to be recorded only once on the photographic plate, and interferograms can be recorded on the much cheaper photographic film.

The **application of holographic interferometry in simultaneous measurements of temperature and concentration fields** has been examined in the work of Panknin (1977). The method is based on the dependence of the refractive index on the wavelength of light — and it was used in the evaluation of both temperature and concentration fields from two interferograms taken at different wavelengths. The optical setup for the two wavelength interferometry, which enables the taking of two interferograms with different wavelengths on the same photographic plate, is presented in figure 12. One He-Ne laser (λ_j) and one argon laser (λ_k) were used as light sources. In the optical setup, two object and two reference waves are formed at different wavelengths. Temperature and concentration fields were measured in the vicinity of a heated vertical plate coated with a thin layer of naphtalene (figure 13). Interferograms were obtained by using the double exposure technique and the modified real-time method. In figure 14, two interferograms, taken simultaneously at different wavelengths, and the evaluated temperature and concentration profiles in the boundary layer are presented. The evaluation technique has been discussed in detail by Panknin (1977) and Mayinger and Panknin (1974).

In the literature, many variations and *modifications of the basic techniques* of holographic interferometry have been discussed. The purpose of these changes is the improvement of the accuracy and the sensitivity of the method. The dual-reference-wave holographic interferometer, the shearing interferometer, the multiple-pass holographic interferometer, the two-wavelength interferometer, etc. are some of the commonly used configurations. Also, heterodyne holographic interferometry (Dändliker (1980), Farell et al. (1982)) has been applied in the study of transport phenomena. The interested reader can find a detailed description of these techniques in the references treating general topics in holographic interferometry cited at the beginning of this section.

Holographic interferometry has become a method widely accepted in the study of transport phenomena. Its applications in flow visualization

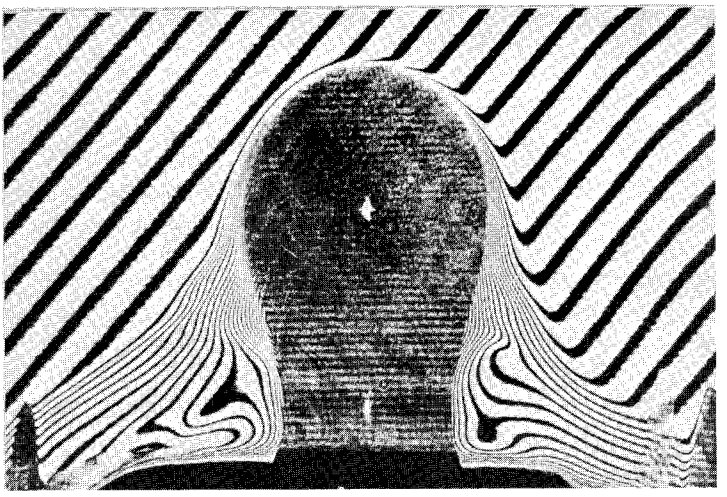

FIGURE 15. Temperature fields of a bubble condensing in liquid (Mayinger and Chen (1986)).

were analyzed by Merzkirch (1987). Application examples in convective heat transfer are numerous, and the references in this paper, because of the limited space available, stand for many others: Panknin (1974), Jahn (1975), Becker and Grigull (1977), Nordmann (1980), Chen (1985), Mayinger and Chen (1986), Ostendorf et al. (1986), Ostendorf and Mewes (1988). A comprehensive overwiev of applications of holographic interferometry in heat and mass transfer was given by Mayinger and Panknin (1974) and Sernas (1983), and in two phase flow by Mayinger (1987).

3.5 STREAMING BIREFRINGENCE

The effect of birefringence — due to the optical unisotrophy of the transilluminated medium — has been observed for transparent solid materials, mainly crystals, and also for some liquids or liquid solutions in the presence of shear forces. The light passing through the birefringent material is separated into two linearly polarized components with perpendicular polarization planes. The two components have different phase velocities (characterized by different values of refractive indices), and the difference in the optical phase at the exit of the test section can be visualized using interferometric methods.

The effect of birefringence can be observed in liquids having elongated deformable molecules or containing elongated particles. When these molecules or particles are randomly distributed (fluid at rest), the fluid is optically isotropic. Due to shear forces, the molecules or particles align in one direction, and the fluid shows birefringent properties. The interference images obtained by this method form an isochromatic fringe pattern, from which ve-

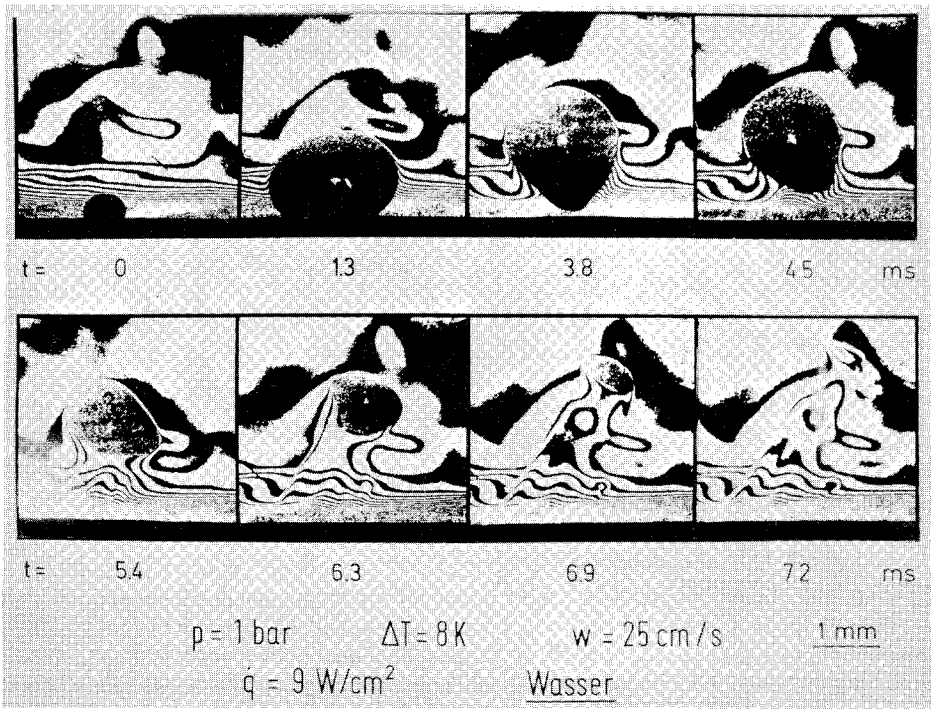

FIGURE 16. Interferograms of boiling water (1 bar, 8 K subcooling) obtained by high-speed cinematography (Mayinger and Chen (1986)).

locity fields can be evaluated, usually by complicated numerical procedures. For quantitative evaluation, the relation between the visualized refractive index field and the flow situation should be known.

Optical arrangements, like polariscope, modified Mach-Zehnder interferometer, scattered light technique, enabling flow visualization by streaming birefringence, as well as application possibilities, were discussed by Philippoff (1961), Janeschitz-Kriegel (1983), Pindera (1983), Johnson and Fuller(1986) and Merzkirch (1987). The method is sensitive to use in the low velocity range, where other methods fail to provide results of sufficient accuracy.

3.6. SPECKLE METHODS

3.6.1 Introduction

Diffusely reflecting or transmitting objects illuminated by laser light appear to have an image of granular structure, consisting of fine, randomly distributed, high contrast dark or light *speckles*. Their origin can be explained as follows. The light scattered by one object point interferes with light scattered by other object points, forming a random pattern of interference fringes called speckle. In most situations (like interferometry or holography), laser speckle sets the limits to the performance of the system (being con-

sidered as optical noise), as it is in the range of the theoretical resolution limit of the system. On a later stage of the application of optical methods in measurement, research efforts were directed towards the use of laser speckle as information carrier, characterizing the scattering medium.

Numerous applications of speckle methods in the measurement of in plane translation, rotation, vibration and surface deformation have been reported in the literature (for further references see Ennos (1978), Vest (1979), Jones and Wykes (1983), and others). In the past ten years, in laboratories throughout the world, these methods are being adapted to measurements in transport processes (refractive index, temperature and density measurements in fluids, velocity field measurements in complex flow fields). Further efforts in this direction are encouraged by the availability of moderate cost image processing systems for easier evaluation of images obtained by speckle photography.

In the literature, several measuring techniques based on the speckle effect have been described, and, according to the effects exploited and the optical arrangement used, two basic methods should be distinguished: (i) speckle photography and (ii) speckle interferometry. In speckle photography, speckle patterns are recorded photographically on plate or film, and used as diffracting structures in the evaluation. Flow visualization by speckle photography is known as laser speckle velocimetry: here, the actual speckle displacement caused by the movement of small scattering particles is measured. In speckle photography of refractive index fields, virtual speckle displacement, caused by the refraction of scattered light, is measured. In speckle interferometry, the interaction of coherent light emanating from a speckle field and a reference beam is exploited. These methods will be discussed in some detail in this chapter, and their application illustrated to the extent allowed by the space available.

3.6.2 Speckle photography

3.6.2.1 Laser speckle velocimetry

In laser speckle velocimetry, the effect of speckle displacement is used to measure flow velocity of the fluid seeded with tracer particles. The method allows, depending on the reconstruction technique, quantitative measurement of fluid velocities in each point of the flow field illuminated by a light sheet and visualization of the velocity fields in the form of iso-velocity lines.

The **physical principles** of the method are illustrated in figure 17. The object point imaged onto the recording plane is photographed at an initial moment, and after a small displacement ds corresponding to a time interval dt. The displacement is proportional to the velocity v ($ds = v\ dt$). Thus, image points of tracer particles are recorded twice on the specklegram. The time interval between the two exposures is known, and by measuring the displacement ds, the velocity of the particle can be evaluated. The displacement is determined by reconstruction of the double exposure specklegram, illuminating it with the unexpanded laser beam (*point-by-point evaluation,* figure 17b). If the seeding rate of the flow was low, the unexpanded laser

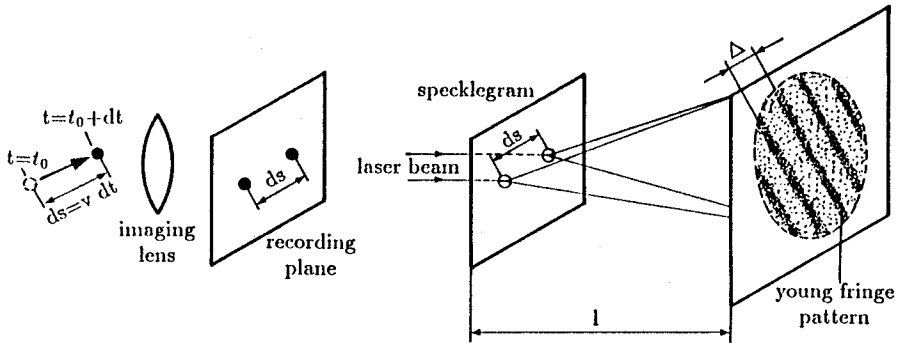

FIGURE 17. Recording the displacement of an object point (tracer particle) on the specklegram by the double exposure method (a) and point-by-point reconstruction of the specklegram by the unexpanded laser beam (b) (Merzkirch (1987)).

beam illuminates individual images of tracer particles, as presented in figure 17, and this situation is called particle imaging velocimetry. At higher seeding rates, patterns obtained in the process of multiple interference of light scattered by tracer particles are registered on the photographic material, and the result of the recording is a real speckle pattern. The two images of the particle in figure 17b behave as point light sources, and emit light into two cones behind the specklegram (halo). The coherent light waves from the cones interfere, forming a pattern of parallel, equally spaced fringes, called Young's fringes, with fringe orientation normal to the displacement ds. The fringe spacing Δ can be measured, and it is defined by the relation

$$\Delta = \frac{l\,\lambda}{ds},$$

with l as the distance between specklegram and the observation plane and λ as the wavelength of light. Thus, by measuring fringe spacing, the displacement and the velocity of the particle can be evaluated. From the fringe pattern, the direction of the displacement cannot be determined. This problem can be solved by means of a small additional displacement of the specklegram between the two exposures.

In the experiments, the illumination is usually managed by a light sheet, as illustrated in figure 18. A double pulsed ruby laser is well suited as light source: pulse duration and the time interval between pulses can be adjusted, in order to achieve optimal experimental conditions, corresponding to the displacement values to be measured. Even when using powerful light sources like pulsed ruby lasers, providing sufficient light intensity for measurement of high speed phenomena, still remains a problem (Merzkirch (1987)).

Apart from point-by-point measurement of the velocity components, laser speckle photography enables the visualization of the velocity field in form

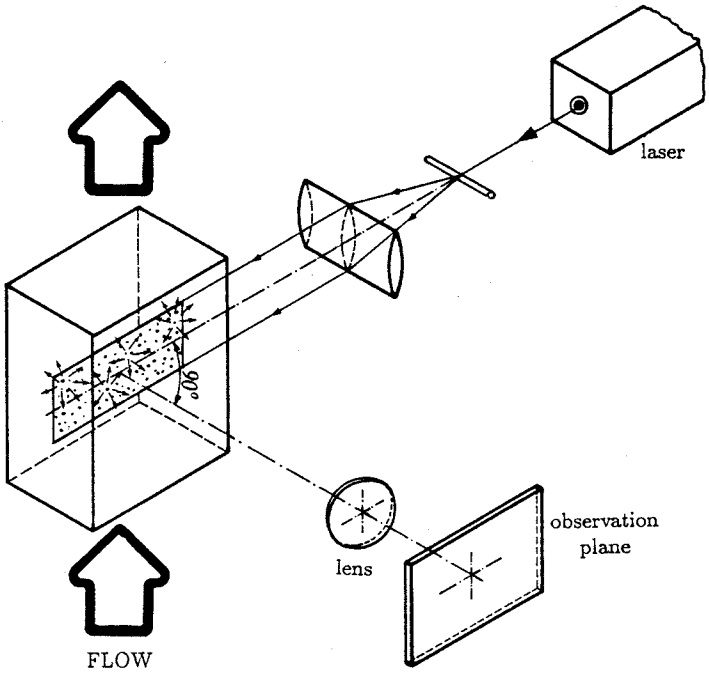

FIGURE 18. Schematic of the setup for generating a light sheet.

of equi-velocity fringes by *spatial filtering of specklegrams*. The principles of spatial filtering are illustrated in figure 19. The specklegram is illuminated by the expanded laser beam, and imaged by means of a lens onto an opaque screen with a hole at an off-axis location. A small amount of light passes through the hole, and is imaged onto the observation plane by the imaging lens. Here, a fringe pattern can be observed, corresponding to equi-velocity contours (figure 20).

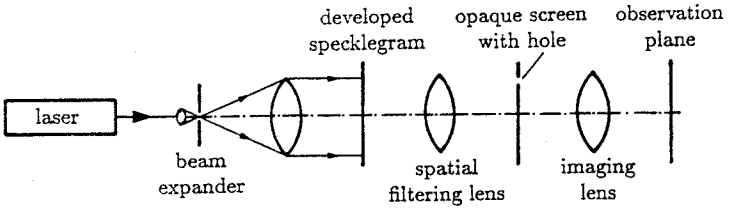

FIGURE 19. Principles of reconstruction of a specklegram by spatial filtering.

It should be noted, that the above description is valid for idealized situations. Using the light sheet method, only two velocity components can be recovered. If a tracer particle is moving in the direction normal to the

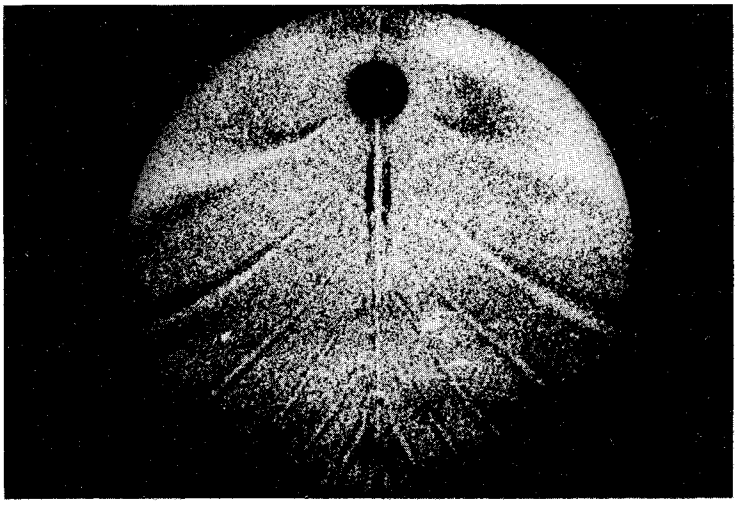

FIGURE 20. Equi-velocity fringes obtained by spatial filtering of the specklegram: velocity field of an internal gravity wave behind a cylinder moving through stratified saltwater (Gärtner, Wernekinck and Merzkirch (1986), with permission of the authors).

light sheet, it may appear as a single image on the specklegram, and, in this case, the degree of correlation of the fringe pattern is smaller. In figure 21, a typical Young's fringe pattern is presented. Limitations imposed on particle size and concentration are discussed in detail by Merzkirch (1987).

Applications. Hinsch, Mach and Schipper (1983) have analysed the *velocity fields in a Kármán vortex street,* produced by introducing a wire into the flow in a wind tunnel. They obtained measurements both in particle imaging mode and speckle photography. Kawahashi et al. (1986) have applied white light speckle photography to investigate the *wake flow field produced by towing of a cylinder in an open channel.* The same authors have measured *two-dimensional velocity distribution of the flow in a peristaltic pump.* In the point-by-point reconstruction they used a He-Ne laser, and spatial filtering was performed using a white light source. Gärtner, Wernekinck and Merzkirch (1986) have used speckle photography in forward scattering to measure and to visualize two dimensional *velocity fields in an internal gravity wave* (figure 20). The wave was caused by a cylinder towed through stratified saltwater. They used neutrally buoyant particles, uniformly distributed, as tracers. Brandt and Merzkirch (1988) measured *droplet velocity in a spray jet* exhausting from an atomizer nozzle by laser speckle velocimetry. In this application, light scattered from water droplets (instead of tracer particles) was used for the measurements. Thus the scatterers were larger as conventional tracer particles and the measured velocities high compared to earlier applications.

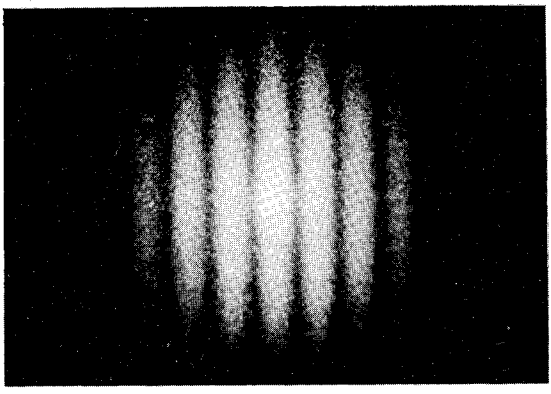

FIGURE 21. Typical Young's fringe pattern (Photograph W. Merzkirch, with permission of the author).

3.6.2.2 Measurement of refractive index fields

Physical principles. The method exploits the effect of speckle displacement, caused by light refraction in a fluid, to measure refractive index and density/temperature fields. The recording is executed in two steps. First, a diffusing object (for example a ground glass plate) is illuminated by laser light, and, in the recording plane, a random speckle pattern is generated by the imaging lens. After recording it in the first exposure, the investigated refractive index field is placed into the path of the parallel laser beam. The light beams generating the speckle pattern are thus refracted, causing speckle displacement from the initial location (without the test field). The displaced speckle pattern is recorded again onto the same photographic plate. After the development, the specklegram can be evaluated point-by-point.

The basic optical arrangement for recording specklegrams for measuring refractive index fields is presented in figure 22. The test section can be placed either behind or in front of the diffuser; the advantages and disadvantages of both techniques have been discussed by Wernekinck (1985). The reconstruction of specklegrams can be accomplished by *point-by-point analysis* (figure 17b) or by *spatial filtering* (figure 19). The evaluation procedure was described in detail by Wernekinck (1985).

The main advantages of speckle photography over interferometric methods can be summarized as follows: (i) the optical setup is simple, (ii) requirements concerning mechanical stability are less stringent, (iii) in speckle photography there is no need for a reference beam, (iv) specklegrams have higher information density than interferograms, (v) speckle photography can be realized with a white light source, (vi) the sensitivity of the method can,

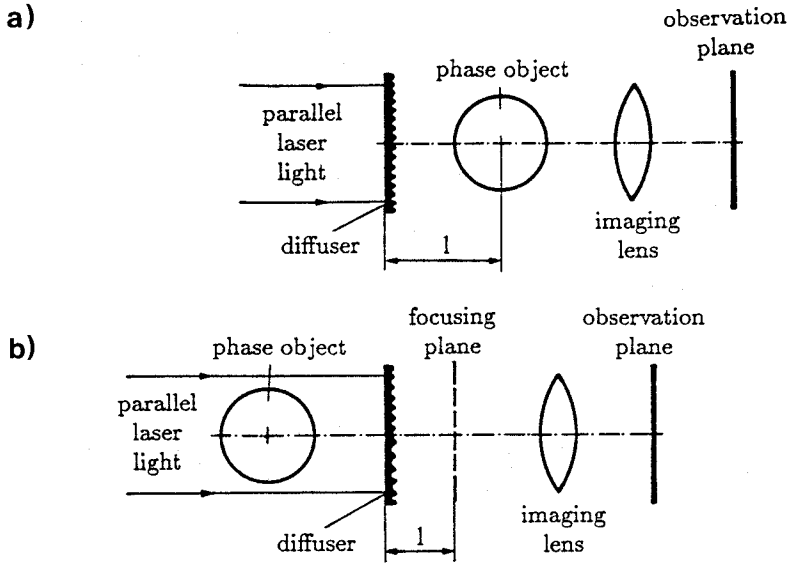

FIGURE 22. Schematic of the optical arrangement for recording the specklegram of a phase object: (a) phase object behind the diffuser, (b) phase object in front of the diffuser (Wernekinck (1985)).

to a certain extent, be adjusted to the problem under investigation.

Applications. *Temperature fields of a propane gas burner* were measured by Farrel and Hofeldt (1984) using speckle photography. The results show good agreement with thermocouple measurements. Wernekinck (1985) has measured the *refractive index field in laminar and turbulent flow of a helium jet exhausting vertically into ambient air* by means of speckle photography, as well as *heat transfer in laminar free convection from a vertical heated cylinder and a vertical heated flat plate* (Wernekinck and Merzkirch (1987)). The results obtained by speckle photography were compared with measurements obtained by schlieren-interferometer and Mach-Zehnder interferometer, and they showed very good agreement. Erbeck (1986) and Erbeck and Merzkirch (1988) have applied speckle photography to the *measurement of turbulence in a mildly heated turbulent air stream* in a low speed wind tunnel. Isotropic turbulence was assumed, and correlation functions were calculated for three dimensional turbulent temperature/density fields. The measured values were compared with data obtained by cold wire measurements. Guo, Song and Zhao (1988) have measured *heat transfer characteristics in laminar natural convection between two isothermal vertical flat plates* in air. In figure 23, a typical set of Young's fringe patterns, reconstructed from a double exposure specklegram for this physical situation, is presented. From the specklegrams, temperature gradients can directly be evaluated: the direction normal to the Young's fringes corresponds to the direction of the temperature gradient, the

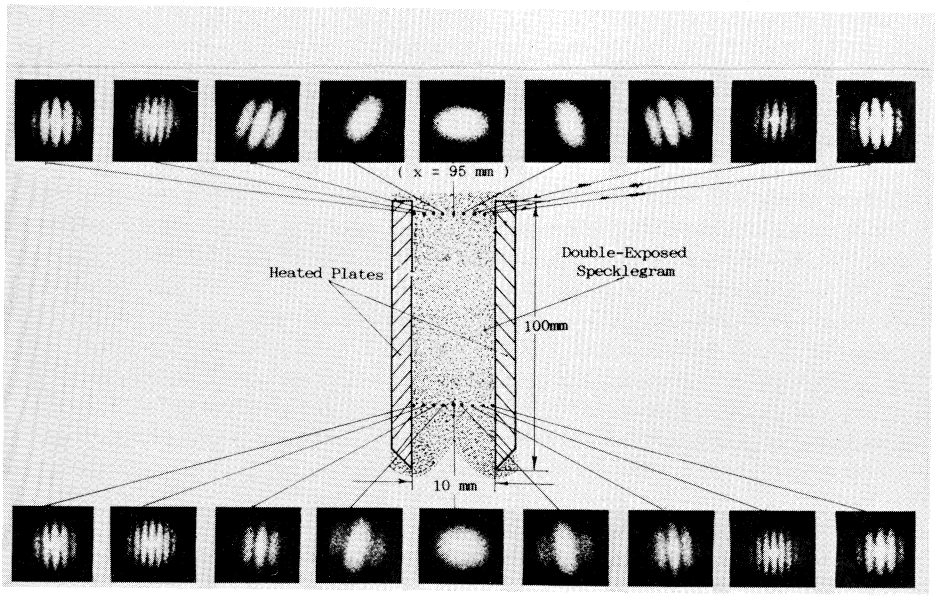

FIGURE 23. Set of Young's fringe patterns reconstructed from a double exposure specklegram of laminar natural convection heat transfer between vertical flat plates (Guo, Song and Zhao (1988), with permission of the authors).

density of the fringes is proportional to the temperature gradient.

3.6.3 Speckle interferometry

Physical principles. Speckle interferometry is a measurement technique which exploits the effect of interference of one speckle field with a plane reference wave or another speckle field. A detailed description of the method can be found elsewhere (Ennos (1978), Vest (1979), Jones and Wykes (1983), Verhoeven and Farrel (1986)).

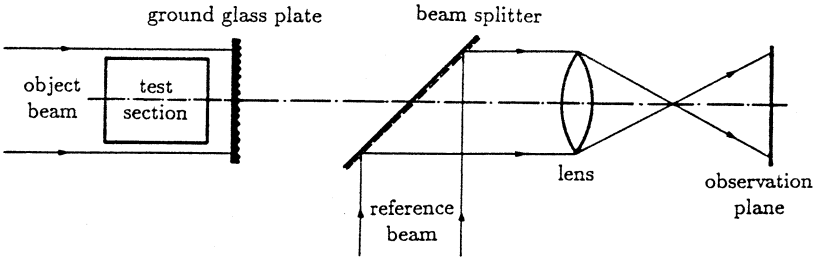

FIGURE 24. Optical arrangement for measuring refractive index fields by speckle interferometry (Farrel and Verhoeven (1987)).

Speckle interferometry measures the changes in the correlation of two speckle patterns. The basic optical arrangement for recording is presented in figure 24. In measurement of refractive index fields, speckles are generated

by a diffuser plate, positioned into the light path after the test section. After traversing the test section, the object beam is diffused by a ground glass plate, and imaged by a lens onto the observation plane, through a beam splitter. The beam splitter combines the reference beam and the object beam — after which the reference beam is also imaged onto the observation plane.

Speckle interferometry is a double exposure technique, similarly to holographic interferometry. The first exposure is taken with the test object at a reference state, and the second exposure in the conditions to be measured. The speckle pattern, generated by the light beam passing through the test section, is described in terms of its intensity probability density function. If the refractive index value in the test section changes between the two exposures, a slight phase change of a portion of a speckle pattern will occur. The combination of the two speckle patterns will result in a fringe pattern with dark and light fringes for correlated and uncorrelated regions of the two patterns. Thus, by evaluating the fringe pattern, information regarding the changes in the refractive index field between the two exposures is obtained. The evaluation procedure of fringe patterns obtained by laser speckle interferometry is similar to the evaluation of holographic or Mach-Zehnder interferograms. Fringes in speckle interferometry are of relatively low contrast, with a general speckle structure superimposed. In order to improve fringe visibility, the optical arrangement shown in figure 25 is used in the reconstruction.

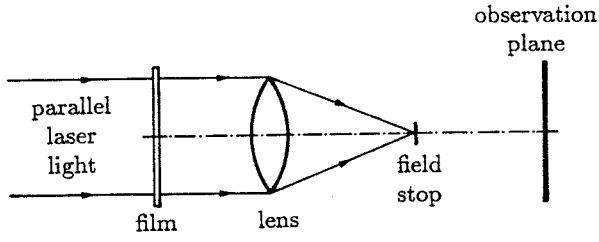

FIGURE 25. Optical arrangement for reconstructing specklegrams obtained by speckle interfreometry (Farrel and Verhoeven (1987)).

Speckle interferometry has certain advantages over holographic interferometry or Mach-Zehnder interferometry; the most important are simplicity, high temporal resolution, reduced sensitivity to vibrations and the possibility to use moderate resolution film material.

Applications. Verhoeven and Farrel (1986) have measured *temperature distributions in a bunsen burner flame.* Measurement data obtained in this way were compared with values obtained by thermocouples, and showed fairly good agreement. *Temperature profiles normal to the cylinder head in a motored two-cycle engine* were measured by Farrel and Verhoeven (1987). The major difficulties encountered were similar as in other image forming techniques — they were mainly due to strong refraction and three dimensional effects.

3.6.4 Conclusions

The numerous applications of speckle methods in measurement of transport processes, published in the literature in the past several years, prove without doubt that these methods are very promising in the study of transport phenomena. They provide continuous information on the investigated phenomenon (velocity fields, temperature fields) with high information density. Accurate quantitative measurements are obtained by means of point-by-point analysis — the specklegram is scanned by the unexpanded laser beam, and the investigated phenomenon can be visualized by spatial filtering. The optical arrangement for speckle methods is relatively simple, the quality of the optical components is not critical, and the whole experimental setup is less sensitive to vibrations than the interferometric arrangement. In the recording, white light sources can be used, and, although most applications required high resolution photographic material (holographic recording material with approximately 2000 lines/mm), applications using moderate resolution film material (200-300 lines/mm) have been reported as well. Light sources needed for illumination still present a problem in the sudy of high speed processes: illumination times must be short, but still provide sufficient light intensity for recording (usually pulsed ruby lasers are used in the recording procedure). The aspects of speckle methods to be investigated in more detail in the future are new application areas, comparative analyses of the accuracies of the speckle methods and "classical" optical methods, suitable light sources and photographic materials.

4. OPTICAL TOMOGRAPHY

4.1 Introduction

The image forming techniques discussed in the previous chapter provide the experimentator with two dimensional information on the process under consideration — along the third spatial coordinate (in the viewing direction) only integrated values of parameters are obtained by transmission methods. As the velocity, temperature and concentration fields are, in general, three dimensional, it is desirable to measure three dimensional data in order to obtain complete information on the investigated phenomenon. This goal can be achieved in local measurements by moving probes through the experimental volume and relating the measurement signals to the spatial location of the probe. Also, by laser-Doppler anemometry, measurements are obtained at only one position at a given moment.

Tomographic techniques, to be discussed in detail in this chapter, enable the reconstruction of three dimensional spatial information on the measurement parameter from two dimensional projections (obtained by image forming methods) in individual layers of the volume under investigation. In recent studies, the tomographic technique has also been applied to the determination of temporally varying, spatially three dimensional field parameters (Mewes et al. (1989)).

4.2 Tomographic techniques for determining experimental parameters

In the tomographic techniques the measurement signals should be related to time and differential volume in space: for this purpose, different kinds of radiation can be used together with the appropriate sensor for detection. The wavelength and the amplitude of the radiation is affected by the properties (like density or refractive index) of the substance under investigation, called field parameters. The reconstruction of temperature, concentration and density fields from field parameters in holographic interferometry has been discussed in the previous chapter for the two dimensional case. The signals of the sensors located outside of the test volume are related to the line integral of the field parameter f as illustrated in figure 26. The mathematical correlation

$$\int_{S_i} f(x, y, z, t)\ ds = \Phi(\rho, \Theta, z, t) \tag{4.1}$$

describes the relationship between the field parameter f and its projections in different directions Θ. In this equation Φ is the measured physical parameter and s is the pathlength through the volume. Depending on the field parameter to be determined experimentally, different physical effects can be exploited in taking such measurements.

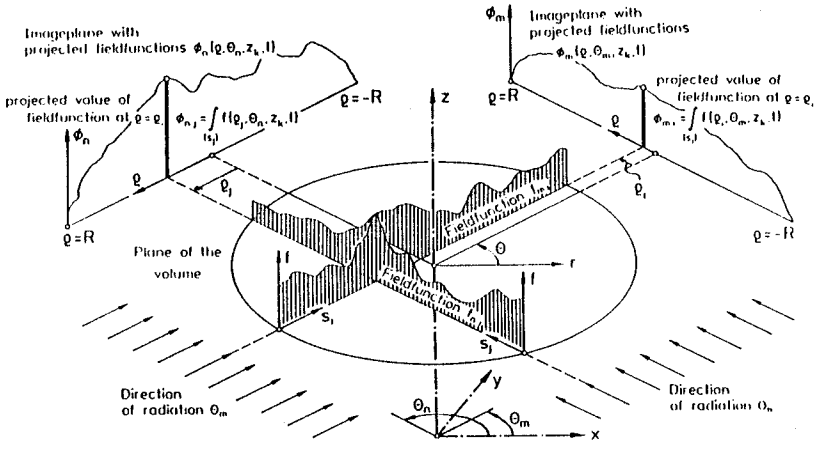

FIGURE 26. Line integrals of the field function along two different paths through the measurement volume.

In the *absorption techniques* the effect of the decrease of radiation intensity during the irradiation of fluids or solids is used, and the field parameter is in this situation the location-dependent absorption coefficient. For measurement purposes, the test volume is irradiated from different directions. The reduced intensity of radiation is visualized as projection using sensors

selected according to the type of radiation. The most commonly used sorts of radiation are X-rays (measurement of density differences in solids or opaque liquids), visible light (concentration differences, temperature, density), infrared light, γ-radiation, corpuscular waves and sound waves (density fields in fluids or solid matter). However, in this study attention will be devoted to methods using light waves.

Three dimensional information on the phenomenon to be investigated can, very conveniently, be obtained by ***holography.*** Chavez (1990a) has described a technique to measure the characteristics of sprays: by appropriate precise positioning and focusing of the imaging lens, he obtained measurement data in several planes of the investigated volume, perpendicular to the viewing direction (this experiment is also discussed in sections 3.3 and 6). It should be stressed here, that in the case of holography, spatially resolved data can be obtained in the viewing direction.

Tomography is frequently combined with *interferometric techniques* which were treated in detail in section 3.4.3. In these methods, the phase shift of the waves passing through the experimental volume is measured. Its application will be discussed in more detail in the case of concentration and temperature field measurement for mixing, later on in this chapter.

Liu, Merzkirch and Oberste-Lehn (1989) have applied optical tomography to the *speckle photographic* measurement of an asymmetric flow field (determination of helium concentration in a helium jet exhausting vertically into ambient air) with variable fluid density. Special attention was devoted to the analysis of the influence of the number of projections used in the reconstruction on the reconstruction quality.

4.3 Mathematical aspects of tomographic techniques

Mathematical methods that enable the evaluation of the unknown field parameter for each spatial coordinate from projections obtained from different irradiation directions, are called tomographic techniques. Because of the limited space available, these methods will not be treated in detail in this paper, but a comprehensive description and further references are given in Kak and Slaney (1988), Hesselink (1989), Hunter and Collins (1989), Mewes et al. (1989) and Mewes and Renz (1990).

Grid method. The simplest method to obtain three dimensional data, from mathematical point of view, is the grid method. In this method, the measurement volume is divided into a grid, and a constant value of the field parameter is assumed for each element of the grid. Thus, the integral equation (4.1) is transformed into a summation equation and it is necessary to obtain the solution of a system of equations based on the available sufficient number of linearly independent experimental results. The method is suitable for reconstructing field parameters in small measurement volumes if a very high quality of reconstruction is not required.

Integral transformation methods. In the integral transformation methods, most commonly used in practical applications, the Fourier transform is applied to reconstruct field parameters. They permit fast and ac-

curate calculation and high quality reconstruction of field parameters, but also require many irradiations from a wide range of viewing angles. As for the investigation of unsteady-state processes all projections must be recorded simultaneously, integral transformation methods are recommended for the investigation of stationary objects.

Combined techniques. These techniques join elements of both methods mentioned above. They combine the high quality of reconstruction of the integral transformation methods and the low number of irradiation angles of the grid methods.

4.4 Applications

In recent years computerized tomography is gaining importance in the study of transport processes, and some of the applications will be discussed in this paper.

Measurements in gases

Willms (1983) has used computerized tomography with infrared radiation to measure the *concentration of aerosol particles in air.* The decrease of the intensity of infrared radiation in the measurement volume was detected by photodiodes, and a computer was used to reconstruct the field parameters. Uchiyama, Nakajima and Yuta (1985) analysed the *temperature distribution in flames* using a pyrometer for temperature measurements in infrared emission computerized tomography. Emmerman et al. (1980) and Santoro et al. (1981) have applied tomography to the determination of *concentration profiles of different gases in free jets.* The experimental parameter was the absorption of light in the investigated volume and a He-Ne laser was used for the transillumination of the measurement chamber. Wolfe and Byer (1982) described a tomographic method to measure *air pollution* in an area of 6 km in diameter simultaneously. The total area was subdivided into 200 m long grid cells, and the experimental parameter was the decrease of light intensity due to absorption in air. The light source was a laser beam that rotated and swept the circular measurement area and hit the mirrors and detectors arranged in a concentric circle around the measurement area. *Density fields around rotating helicopter rotor blades* were measured with optical tomography by Snyder and Hesselink (1984). The effect of phase shift of coherent light in the volume under investigation was used. An experimental setup for tomographic measurements of *unsteady-state density and concentration fields* was described by Snyder and Hesselink (1985).

Measurements in liquids

Measurement of *unstationary temperature fields in stirred vessels* using optical tomography has been described by Lübbe (1982), Mewes and Ostendorf (1983), Mayinger and Lübbe (1984), Ostendorf, Mayinger and Mewes (1986), Ostendorf (1987), Ostendorf and Mewes (1988) and Friedrich (1990). The *time- and location-dependent mixing* of a liquid component in a stirred vessel was examined using two liquids of different temperature and identical concentration. Temperature fields were simultaneously recorded from four directions using holographic interferometry (finite fringe field arrangement)

in real time mode.

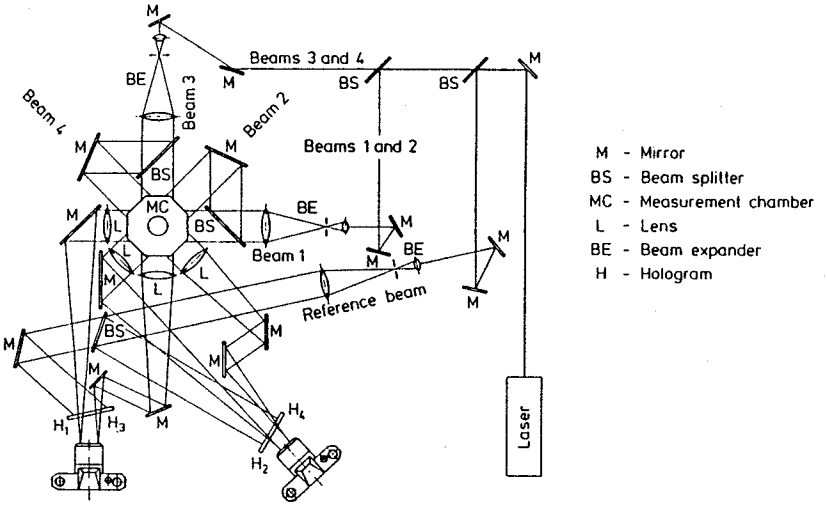

FIGURE 27. Experimental facility for optical tomography with holographic interferometry used in the measurement of temperature in stirred vessels — proposed by Lübbe (1982).

The optical setup used in this investigation is presented in figure 27. The light beam of an argon-ionen laser is separated into an object beam and a reference beam by means of a beam splitter. Another beam splitter divides the object beam into two portions, and each of them is divided again into two object waves after having passed through two beam expanders. Thus the measurement chamber is irradiated at displacement angles of 45°. After passing the test volume, the object wave is bundled by lenses in order to increase the light intensity on the holographic plate. The reference beam is also projected onto the holographic plate after passing through a beam expander. Interferograms are photographed by motor driven cameras with synchronized shutter release. The measurement chamber consists of an octagonal exterior vessel and the cylindrical stirred vessel installed into the centre of the tempering vessel. Both the exterior vessel and the stirred vessel are filled with liquid which has the same index of refraction as the applied glass. Turbines with six blades and a simple cylindrical disk were used as stirrers. The mixing of liquid volumes of different temperatures (a small volume of the same liquid but with different temperature is injected into the stirred vessel) is investigated. The interference pattern has even stripes before the adding of the warm liquid (finite fringe field arrangement). The temperature change during the mixing process can be evaluated from the deflection of the interference stripes for each plane of the vessel. In figure 28, a temporal sequence of six interferograms is presented. Typical reconstructed temperature

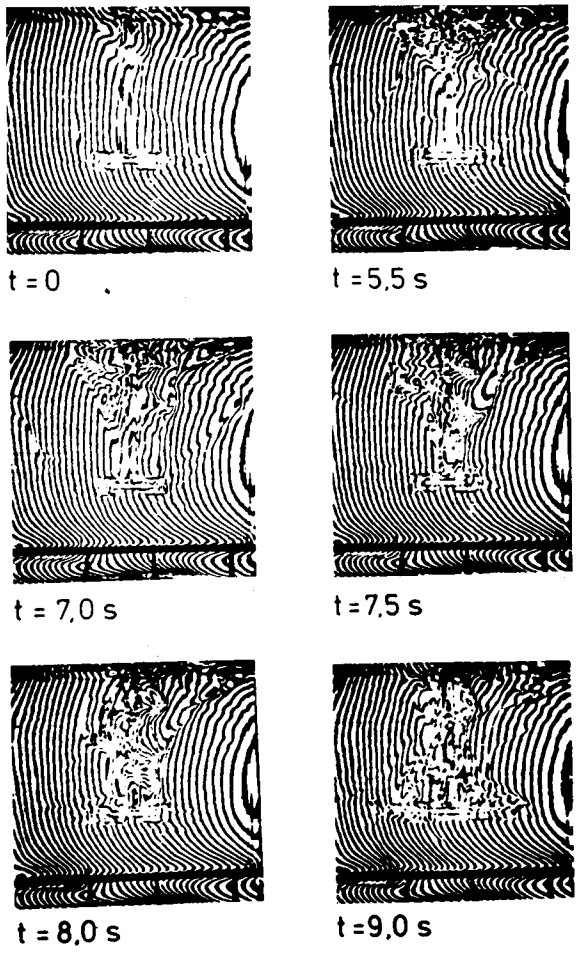

FIGURE 28. Interferograms of a mixing vessel photographed at different instants of time with finite fringe field alignment. At the top of the vessel a small fluid volume of different temperature is injected (Ostendorf (1987)).

fields are shown in figure 29. With the same optical setup Ostendorf (1987) has measured dissipation in laminar mixing.

Concentration fields in a jet-mixed vessel were measured by Haarde (1989). In the experiments, concentration profiles of a dye, corresponding to the steady-state mass exchange process during jet mixing, were observed. The dye is either injected, or it develops during a color change reaction. The test volume is illuminated from four different directions (each closing an angle of 45° with the neighbouring light bundle and thus covering the range of 180°) via mirrors and beam splitters. With cylindrical lenses, the vessel

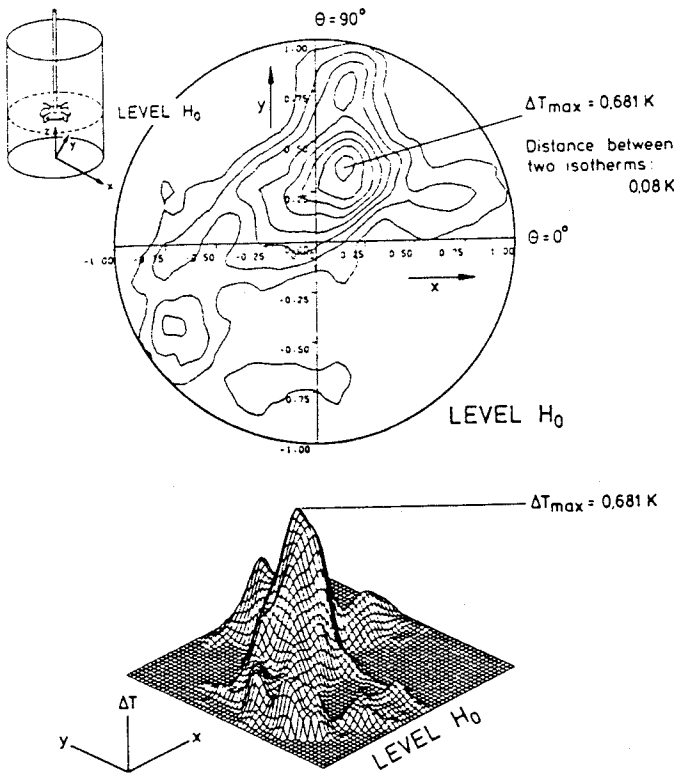

FIGURE 29. Temperature profiles in one cross section of the mixing vessel computed by the tomographical method (Lübbe (1982)).

was illuminated in sections of $50mm$ height each, and the vessel, $200mm$ high and $200mm$ in diameter, was divided into four sections, in order to cover the total experimental volume. After having passed the volume under investigaton, the light falls onto ground glass plates and the image formed on these plates is photographed with synchronized cameras. A typical image, composed of the pictures taken at different heights, is presented in figure 30. The decrease of light intensity during the mixing process was measured from the photographic film, and three dimensional concentration fields were reconstructed tomographically from the four projections.

4.5 Conclusions

Optical tomography is a complex technique which enables the reconstruction of three dimensional data from two dimensional images photographed from different viewing angles. Both the experimental and the numerical effort necessary to obtain 3D reconstructions of desired accuracy, is significant, but, with the availability of powerful computers and image processing systems at acceptable prices, these techniques are brought closer to enginee-

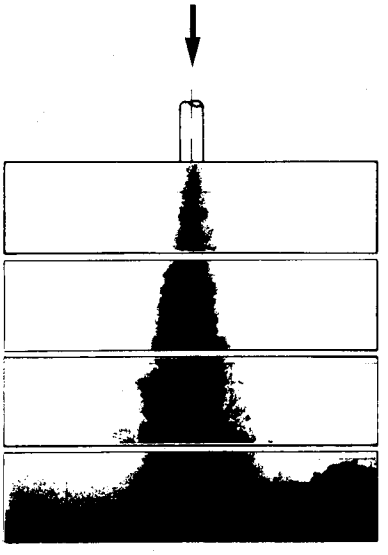

FIGURE 30. Photograph of the jet-mixing process from one viewing direction. The decrease of light intensity during transillumination is proportional to the concentration Haarde (1989).

ring applications — where their possibilities are far from being exhausted.

5. LOCAL MEASUREMENTS

In local measurements, temporally continuous, spatially discontinuous data on the investigated phenomenon are recorded by the optical sensor. This sensor can either be realized as an optical probe or as a light beam focused to a small volume in space, with corresponding receiver optics focused to the same point of the volume. Two dimensional or three dimensional information is obtainable either by mechanically traversing the test volume with the optical probe, or by using a matrix of electro-optical receivers to convert the visual information in the recording plane. In the following sections, optical methods based on light scattering will be discussed in some detail, and one example of measurements by means of optical probes — as the construction of optical probes is application specific — in two phase flows will be introduced in section 5.2.

5.1 MEASUREMENT TECHNIQUES BASED ON LIGHT SCATTERING

On irradiating the fluid with laser light, an energy interaction between laser photons and fluid molecules, tracer particles, aerosols ... can be observed. Speckle velocimetry also uses the effect of light scattering to measure the velocity of tracer particles, but in the methods treated in this section, the information contained in scattered light is evaluated, in order to extract quantitative data on fluid velocities, temperatures, densities, etc. Different scattering effects can be observed, and the process itself is strongly dependent on the characteristics of light and those of the scattering centres. In Mie scattering exploited in laser-Doppler anemometry, light is scattered from tracer particles introduced into the flow; fluorescence, Rayleigh and Raman scattering are typical molecule sensitive light scattering techniques. An overview of the methods treated in the paper is presented in table 2.

Measuring technique	Scattering process	E - Elastic I - Inelastic	Scattering centres	Measured parameter
Laser - Doppler anemometry	Mie scattering	E	tracer particles	particle velocity, size
Laser induced flourescense	Flourescense	I	atoms molecules	atomic and molecular density, temperature
Raman spectroscopy	Raman scattering	I	molecules	molecule - concentration - structure - temperature

TABLE 2. Characteristics of light scattering measuring techniques used in the study of transport processes.

The first applications of scattering techniques were restricted to local measurements, and a typical optical setup is discussed in the section on laser-Doppler anemometry. In local measurements, by accurate focusing, high spatial resolutions can be achieved in addition to the high temporal resolutions characteristic for the methods. On the other hand, in the past years two dimensional applications using scattering techniques have been reported (reviewed by Leipertz and Knapp (1984)). In the experimental setup, a thin light sheet (50 to 200 μm) is generated (like in figure 18) and scattered light is generally collected perpendicular to the plane defined by the light sheet. The spatial resolution of the system depends on the dimensions of the matrix and the digitalization format.

5.1.1 Laser-Doppler anemometry

The first applications of laser-Doppler anemometry (LDA), also called laser-Doppler velocimetry, in the measurement of fluid velocity in air and other transparent fluids, date from the late sixties. Laser-Doppler anemometry delivers the experimentator local measurement data on fluid velocities by measuring the velocity of tracer particles (the properties of particles chosen in such a way, that their velocity would coincide with the flow velocity) introduced into the flow. The physical effect exploited in the measurements is the Doppler effect, a frequency shift received by a fixed observer when electromagnetic waves emitted from a fixed source are reflected from a body in motion. The apparent change of frequency (Doppler shift) f_D is related to the velocity of the moving object according to the relation

$$\frac{f_D}{f} \sim \frac{v_r}{c}, \tag{5.1}$$

with v_r as the velocity of the object reflecting the light waves, and c as the velocity of light. As the ratio v_r/c is usually much smaller than unity, the frequency shift to be detected is very small. The discovery of lasers, sources of electromagnetic radiation with extremely narrow bandwidth, enabled the use of the Doppler effect in the measurement of flow velocities low compared to the velocity of the light.

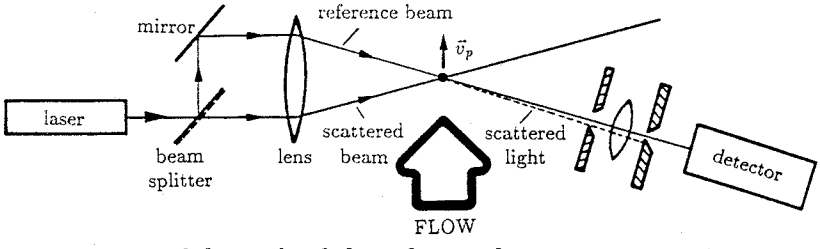

FIGURE 31. Schematic of the reference beam arrangement.

Different optical arrangements can be used to measure fluid velocities in laser-Doppler anemometry, and here two of them will be explained briefly, in order to illustrate the principles of this measuring technique. In the *reference beam arrangement* (figure 31), the laser beam is split into two parts with different intensities. Both beams are focused to a point in the measurement volume by a lens. The optical detector converting optical signals into electric signals is also focused to this point, and receives scattered light (from tracer particles traversing the measurement volume) in the direction of the weak reference beam. The signals received from the photodetector are proportional to the Doppler shift. The disadvantage of this optical setup is the low signal intensity, due to the fact that scattered light is received only from this one direction. It is eliminated in the *dual scatter arrangement* (figure 32) which is commonly used in commercial systems nowadays. In this setup, scattered

light from a whole sector is focused by a lens and received by the detector. The Doppler signal is proportional to the difference in the frequencies related to the light scattered from the two beams.

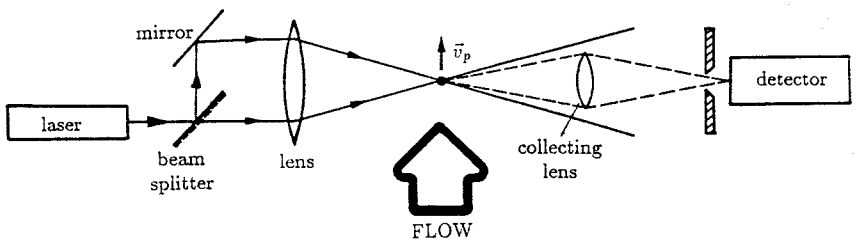

FIGURE 32. LDA: dual scatter arrangement.

The theory of Mie scattering and the Doppler-effect, as the basis of LDA measurements, is very comprehensive, and for a detailed description the reader is referred to specialized literature (Goldstein, Kreid (1976), Wiedemann (1984), Durst, Melling, Whitelaw (1987)). In this paper, only a simplified model called the fringe model will be used to explain the physical principles of LDA. They are illustrated in figure 33, showing the intersection of the two laser beams at a given angle Θ. The two coherent light beams interfere, forming a three dimensional fringe pattern in the intersection region. The tracer particle passes these light and dark fringes and scatteres light at a frequency that is directly proportional to the component of the particle velocity normal to the fringes and inversely proportional to the fringe spacing. According to this theory, the Doppler signal appears due to amplitude modulation in the scattered light. The optical signals are received by a photodetector and converted into electric signals, which are then analysed and evaluated by complex electronic equipment.

Different LDA constructions have been developed by the manufacturers of these instruments; the physical process to be analysed and the parameters to be measured are usually governing the choice of the system. LDA systems operating in forward scattering mode have the advantage of high signal intensities (so that even small scattering particles can be used), in back scatter systems, the emitter and the receiver optics are on the same side, for easier adjustment and scanning of the test volume. In order to gain information on the direction of the velocity vector, a frequency shift is introduced into the optical signal by a Bragg cell. Two velocity components can be determined from several measurements with simple single channel systems in the case of stationary flows. Two or three velocity components can be measured simultaneously by two channel or three channel setups.

The advantage of LDA over "classical" velocity measurements, like hot wire anemometry, is that information is transmitted into and out of the flow by light beams, so that the method is nonintrusive. Thus, measurements of recirculating flows, laminar flows close to the critical Reynolds number, measurements in narrow channels and measurements of fluctuating and highly

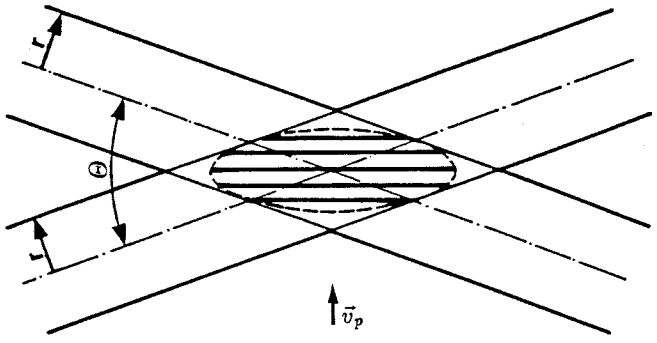

FIGURE 33. Physical principles of LDA — fringe model.

turbulent flows, etc., became possible. In two phase flows, it is possible to measure particle size and particle concentration using LDA, by analysing the modulation of the signals. LDA can be used in corrosive fluids, extreme environments and in fluids where the contamination of conventional probes causes degradation of measurement accuracy. In LDA measurements, there is no need for calibration, as the relation between the Doppler frequency and particle velocity is exact. By accurately focusing the light beams, the measurement volume can be kept small, and, in this way, high spatial resolutions can be achieved for measurements in boundary layers. LDA is a robust measurement technique also suitable for industrial applications.

The key disadvantage of the method is that velocities of tracer particles are measured, not fluid velocities; in some flow situations these tracer particles do not follow exactly the fluid flow. Adding tracer particles into the flow can sometimes be connected with technical problems. Uncertainities regarding the location of the measurement region are present, due to the absence of mechanical probes. In simple measurements, the cost and complexity of the optical equipment and the equipment used in signal analysis can appear as a disadvantage.

Numerous applications of LDA have been reported in the literature in the past years, and the reader can find further references and application reports in the overview literature (Penner and Jerskey (1973), Goldstein and Kreid (1976), Hewitt (1978), Wiedemann (1984), Durst, Melling and Whitelaw (1987), Durst (1988), and others).

Particle Dynamic Analizer, PDA, also called Phase-Doppler Anemometer. Accurate measurement of particle size and concentration is of great importance in scientific and engineering applications: in the study of the properties of nozzles, in combustion and cavitation measurements ... The knowledge of particle dynamics implies the simultaneous measurement of particle size, velocity and concentration distribution. The recently introduced PDA method is very suitable for such tasks: the dynamic range regarding particle size is wide, its accuracy is high, without the need for calibration,

and the system is not sensitive to optical disturbances.

Phase-Doppler anemometry exploits the additional information contained in the phase of scattered light (of the LDA signal), which is related to the size of the particle. The experimental setup is similar to the LDA setup: the receiver cosists of at least two stationary photodetectors with a certain displacement between them. They receive the identical frequency from the scattering particle, but with a certain phase shift. From the measured phase shift, the particle size can be determined. Details about this measurement technique and further references can be found in Saffmann (1989).

5.1.2 Laser-induced fluoresecnce

In laser-induced fluorescence (LIF) measurements, the frequency of the laser used for illumination is tuned to coincide with the molecular absorption line or band of the fluid. On illumination, a transition of the molecule to a higher excited electronic level occurs. The transition is then followed by reemission of light at the same or a shifted frequency. The wavelength of fluorescence differs from the wavelength necessary for excitation, the physical process of fluorescence is thus governed by inelastic scattering. The fluorescence intensity is several orders of magnitude higher than in Rayleigh or Raman scattering.

Fluorescent measurements can be performed in gas flows, combustion processes ..., either by seeding the flow with suitable fluorescending species (like molecular iodine, I_2, atomic sodium, Na, or nitric oxide, NO) or by visualizing and measuring the local concentration of reacting species generated in a flame (resonant wavelengths of OH are used for excitation in such experiments). The experimental configuration in these measurements can be very complex: for example, in NO- and OH- fluorescence measurements the laser system consists of a pulsed dye laser, pumped by Nd:YAG laser and frequency doubled by a wavelength extender unit. LIF enables both flow visualization and quantitative measurements of velocity, concentration, temperature and density, as discussed in more detail in the applications.

Applications. Gross, McKenzie and Logan (1987) have reported an application of LIF which provides *simultaneous measurements of temperature, density and their fluctuations* owing to turbulence in unheated compressible flows. Pressure and its fluctuations were deduced from the equation of state for a non reacting perfect gas mixture. Fluorescence was induced in nitric oxide that has been seeded into nitrogen flow. Measurements were obtained by laser pulses with 1 mm spatial resolution and 125 ns temporal resolution. Hassa, Paul and Hanson (1987) used broadband fluorescence of iodine, excited at 514.5 nm by a single mode argon-ion laser to measure the *velocity of iodine molecules seeded in a nitrogen jet flow.* Walker (1987) used a fluorescence technique to measure *concentration in mixing liquids.* Fluorescent sodium in a buffer solution was used to study jet flows. For further details about the technique and references, the reader should consult the publications of Leipertz and Knapp (1984), Merzkirch (1987), Leipertz (1988).

5.1.3 Linear Raman-scattering

In Raman-scattering, the scattered signals are frequency shifted compared to the frequency of incident light (inelastic scattering). The frequency shift corresponds to the transitions between stationary energy states within the electronic ground state of the molecule, conversely to LIF, with transitions between different electronic states. This shift is characteristic for the species and for the observed molecular energy transition. In Raman-scattering, no requirements are imposed on the laser wavelength needed for illumination. The method is characterized by its insensitivity to disturbances and its specificity, and it is widely applied in density, temperature and concentration measurements in gases. As the scattering cross-section is several orders of magnitude smaller than in fluorescence, signal intensities are low compared to fluorescence. This is one serious disadvantage of the method, and poses a problem in technical and industrial applications. Details about the method, optical setup and applications are given in Leipertz (1981), (1988), (1989), Leipertz and Knapp (1984) and Strube (1990).

5.1.4 Coherent Anti-Stokes Raman Scattering (CARS)

CARS is one nonlinear version of the Raman-scattering technique which overcomes the difficulties caused by low signal intensities in linear Raman-scattering — still keeping the advantages of it. In CARS, the experimental

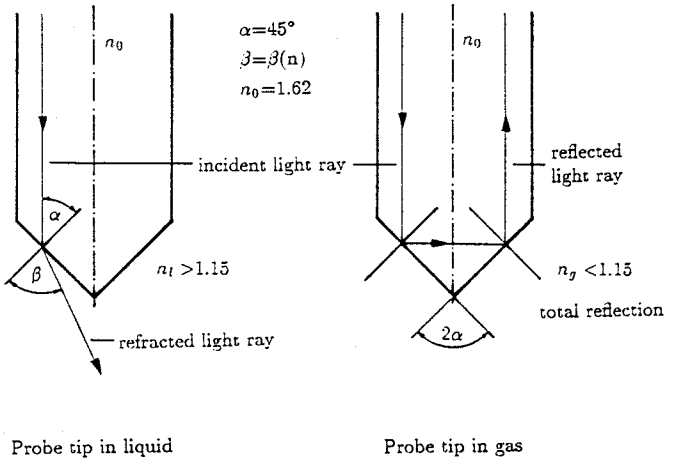

FIGURE 34. Physical principles of the optical fibre probe operation.

effort is high and the evaluation of measurement signals complex: at least two lasers operating at different frequencies are needed, and the measurement location has to exactly be focused with the different laser beams. Because of the high signal intensities, CARS is suitable for industrial measurements. A detailed evaluation of the technique and the possibilities of its applications

can be found in Brüggeman, Hassel and Dittie (1987), Leipertz (1988), (1989) and Stricker (1988).

5.2 OPTICAL PROBES IN GAS-LIQUID TWO PHASE FLOWS

Optical fibre probes are being used for local void-fraction measurements in gas-liquid two phase flows in the past twenty years (Hewitt(1978)). With the corresponding data acquisition equipment for signal processing they deliver temporal and spatial data (local void fraction, bubble frequency, droplet size) on the investigated flow. It is necessary to point out that this optical measurement technique differs from those discussed previously, in the sense that the fibre probe influences/disturbes the flow. Still, such methods are of practical importance also for industrial measurements, as their application area is not limited to transparent or electrically conducting fluids, they can be used in a chemically aggressive medium, etc.

The **physical principles of optical probe measurements** will be explainded on the example of the optical probe developed by Spindler et al. (1988). The effect of refraction of light passing through materials with different refractive indices is exploited in the measurements. The fibre probe is manufactured of materials with the refractive index $n_0 = 1.62$ (commercially available multimode fibre) and its tip is polished into a cone of 90° angle (figure 34).

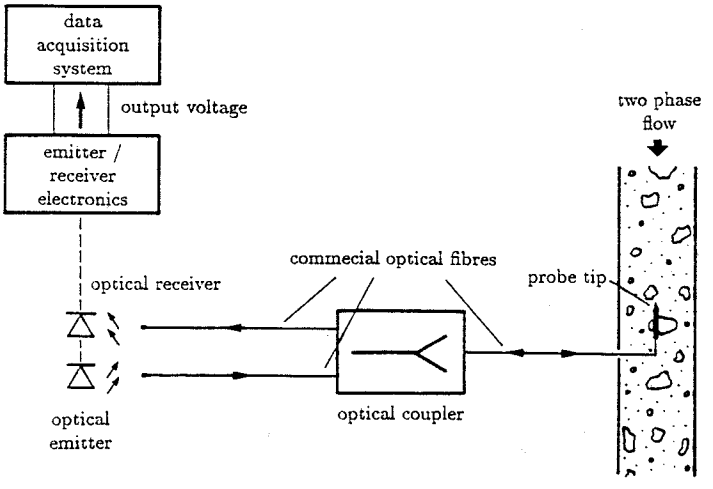

FIGURE 35. Schematic of the setup for fibre probe measurements.

A powerful light emitting diode is used as optical emitter, and a photodiode operates as a receiver, and converts the reflected light into an electric

signal. A bidirectional optical coupler separates the incoming and the reflected light, allowing light to pass in both main directions but not directly from emitter to receiver.

If the gas phase is present at the tip of the sensor, the light is reflected back to the optical fibre. If the probe tip is in the liquid, as illustrated in figure 34, the light beam is refracted, and practically no light reaches the optical receiver. In the optical receiver, the optical signal is transformed into an electric signal. In the signal processing unit, the signal is then amplified, transformed into digital information with different signal processing algorithms, and the desired information is displayed (figure 35). Optical fibre probes have proved to be a useful tool in the study of two phase flows (Auracher, Marroquin (1989), Stephan, Mayinger (1989)). Stephan and Mayinger (1989) have used the same type of probes in vertical countercurrent two phase flow to measure time-averaged droplet fraction. Measurement uncertainities in optical fibre probe methods are due to the specific data evaluation, wetting, break-away and group effects in the probe tip. Developments considering tip size reduction, data evaluation etc. are still necessary.

6. EVALUATION OF IMAGES AND SIGNALS OBTAINED BY OPTICAL MEASUREMENT TECHNIQUES

One important aspect of optical measurements is the evaluation of optical signals. The conversion of visual information into quantitative measurement data, fast data acquisition with the task to cope with the high temporal resolution of the methods, fast manipulation and storage of large amounts of data, are some of the main objectives. For this reason, the equipment for data evaluation is an integral part of the experimental setup.

In local measurements is the evaluation of optical signals decidedly application specific: in the optical detector, the optical information is converted into electric signals, these are usually preprocessed by complex electronic equipment, and afterwards evaluated, presented and stored by the computer. The signal processing operations are designed by the manufacturers of measurement equipment, with certain degrees of freedom left to the operator. A new dimension was introduced into the evaluation of information obtained by light scattering methods by applying multichannel analysers like vidicons or diode array cameras. These, originally local measurements, now enable the visualization of the process in form of two dimensional field information (Leipertz and Knapp (1984)).

The important advantage of the image forming optical measuring techniques, the availability of high density visual information on the complete test field, can turn into a disadvantage when accurate quantitative data on the investigated phenomenon are needed. The evaluation of optical images by hand is, as a consequence of the large quantities of information contained in a single picture frame, a time consuming procedure connected with errors. For this reason, the application of the methods was very often limited to specialized research laboratories. In order to extend their acceptance and their use to industrial measurements, one essential requirement would be the

reduction of evaluation times, the costs connected with the evaluation and the equipment needed for these purposes. Applications of image processing systems for military tasks, in medicine, in radar systems and space techniques are well known, but until recently, they were implemented on large computers, beyond the possibilities of smaller laboratories. The rapid development of computer techniques in the past years enabled the design of image processing applications on low cost personal computers as well.

Image processing can be used in the evaluation of images obtained by holography, holographic interferometry, speckle methods, tomography, and it is particularly important in the study of instationary phenomena. The elements of an image processing system for this variety of applications include typically a video camera (converting visual information into electronic signals) in connection with a digitizer card (responsible for the digitalization of the images) and a computer with a high resolution graphics screen responsible for data storage and manipulation.

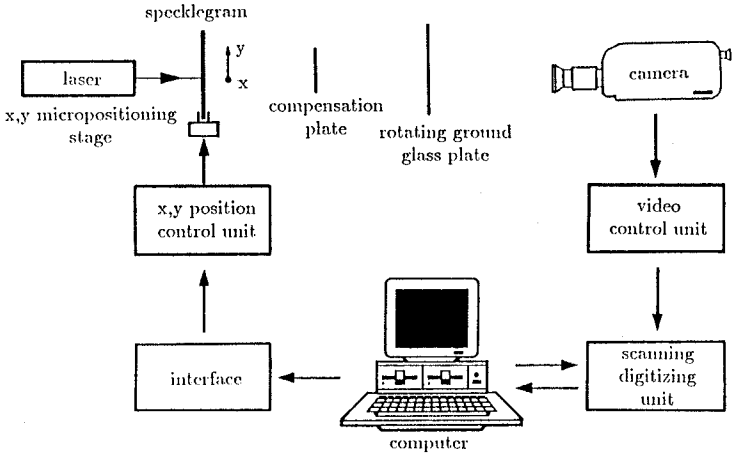

FIGURE 36. Setup for image processing of specklegrams used by Erbeck (1985).

In image processing, the phases of image enhancement (filtering in order to smooth noisy data or to enhance edge detail, altering image data by means of histogram manipulation, skeletonization, grey-level processing...) and image analysis can be recognized. In the first phase, the image is enhanced to a degree necessary to obtain data of sufficient quality for image analysis. Nowadays, software packages performing such transformations are commercially available. The second stage is application specific, with the aim of the interpretation of the image and the investigated physical process. In holographic interferometry, fringe extrema should be detected and located, fringe orders should accurately be assigned to these extrema, and the corresponding density field reconstructed. For this purpose, specialized, often

user specific algorithms have been developed and reported in the literature.

The final goal of all these efforts is the automatition of the evaluation procedure as far as possible and the reduction of the time needed for interpretation. Full automatition is usually difficult to implement because of the complexity of the task. In semiautomatic image analysis, the interactive system allows the operator to alter erroneous locations, reject unsuitable data, align fringes, etc.

Image processing in speckle photography. An image processing system for fast point by point evaluation of specklegrams was developed by Erbeck (1985) and (1986). The arrangement used in the evaluation is presented in figure 36. The specklegram is mounted onto a precision $x - y$ micropositioning stage controlled by a computer. By translating the specklegram in $x - y$ direction, the unexpanded laser beam can sequentially scan the whole image. The Young's fringe pattern is formed on a rotating ground glass plate (it suppresses additional speckle noise generated by the rough surface of the screen), after passing through the compensation plate (reduces the radial mean intensity variation of the speckle pattern). After this optical preprocessing, the fringe pattern is recorded by a video camera. The analog video output of the camera is scanned and digitized to a 180 · 280 pixel matrix, and stored by the comuter. In order to determine fringe direction and spacing, the autocorrelation method was used, the evaluation programs written in machine code to reduce computing times. Evaluation velocities of 2 seconds/picture frame were achieved using an Apple computer with 6502 CPU.

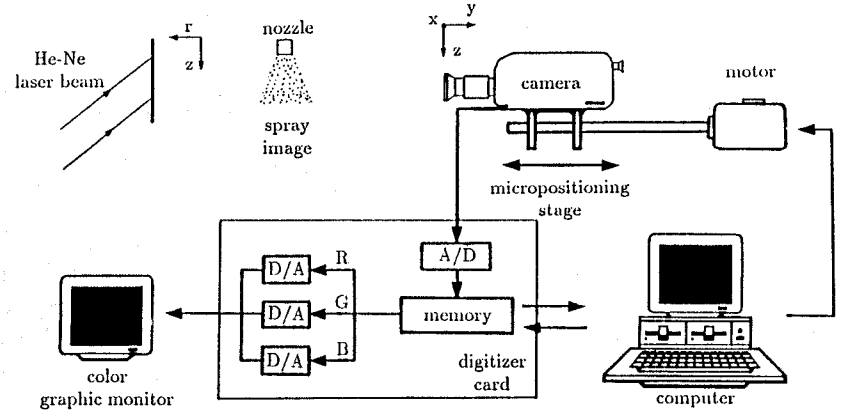

FIGURE 37. Setup for evaluation of holograms of sprays by digital image processing in off-axis configuration (Chavez and Mayinger (1989)).

The researcher is faced with a completely different physical and computational problem when **evaluating pulsed laser holograms in the char-**

acterization of sprays using image processing techniques. The physical problem and the technique of hologram recording and reconstruction has been discussed in detail in chapter 3.3.2 and by Chavez (1990a). In figure 37, the arrangement used in the evaluation by digital image processing is presented (Chavez and Mayinger (1989), Chavez (1990b)). One fundamental difference between this setup and the one used by Erbeck, is the off-axis reconstruction. The hologram is illuminated with the reference beam to reconstruct the image of the spray, and the image can be scanned by using a video camera (the optical axis of the camera and the reconstructed object beam should coincide). As the angle between the reference beam and the holographic plate has to remain constant, the position of the camera is to be varied and controlled in order to scan the whole image. The camera is mounted onto the micropositioning table, and its movements are controlled by the computer. As the camera sensor is only capable of recording two dimensional images, the three dimensional image of the spray has to sequentially be scanned and registered in the form of a series of two dimensional images, each containing data within the range of the depth of the field. The scanning is achieved by accurate focusing and positioning of the camera in the y direction (perpendicular to the image plane).

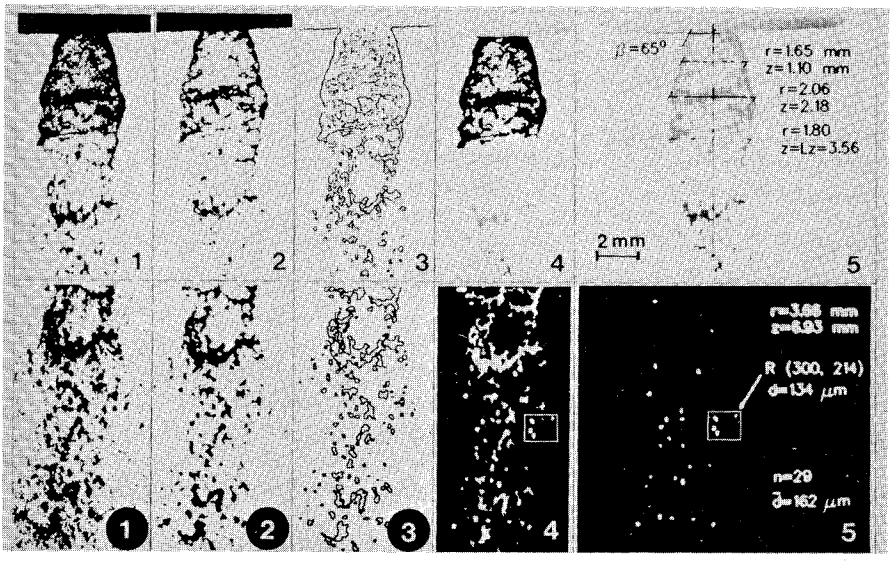

FIGURE 38. Series of images (upper and lower portion of the spray) obtained by image processing manipulations of single- and double pulsed holograms: (1) original image, (2) noise filtering and smoothing, (3) edge recognition, (4) filling with colors, identification of image elements to be measured and (5) results (Chavez and Mayinger (1989)).

The analog signal of the camera is converted into digital information by the digitizer board and stored into the frame memory of the digitizer.

This information is then used by the computer in the image processing manipulations. The results of the manipulations can be viewed on the graphics screen.

Two typical holographic images, subjects of evaluation, are presented in figure 4, and a series of images obtained by different image processing manipulations can be seen in figure 38. The goal of image processing is to (i) recognize image elements representing droplets and separate them from the noisy background, and (ii) to identify well focused droplets and enhance them to a degree that allows the measurement of droplet size. These operations are in the second phase followed by the measurement of (i) the surface of a droplet image, (ii)the determination of its centre of gravity and (iii) the equivalent diameter of the droplet. The algorithms used in these operations are discussed in detail by Chavez (1990b). From double-pulsed holograms, information on droplet velocity can be extracted by identifying droplet pairs after the image enhancement manipulations. In the design of the identification algorithm, preliminary knowledge on the investigated phenomenon and velocity estimates, provide useful information for the operator. After the identification, the distance between the centres of gravity of droplet pairs is measured, and the velocity of the droplet determined. **Other applications.** In the evaluation of interferograms, the subject of the analysis is a complex fringe pattern. Image processing applied to holographic interferometry has been reported by Choudry (1982), Kreis (1986), Hariharan, Oreb and Brown (1987), Hunter and Collins (1987), Osten, Saedler and Rottenkolber (1987).... Further applications of automatic image processing were reported by Inechen, Eglin and Dändliker (1980), Imaichi and Ohmi (1983), Robinson (1983), Huntley, Palmer and Field (1987)...

7. CONCLUSIONS

As the previous pages have shown, optical methods are widely accepted in the measurement of transport processes. New possibilities were opened in the past decades, after the discovery of coherent light sources, the lasers. This discovery was followed by the development of new photographic equipment and recording materials, sensors and electronics needed for the evaluation of optical signals. The dramatic expansion of computer electronics provided tools for the evaluation of visual images by means of image processing. Commercially available optical fibre probes are implemented in measurements. Every day, new applications are reported, and existing measurement techniques are improved. With the development of robust equipment and methods and the reduction of evaluation times and costs, optical methods cease to be confined to specialized laboratories — to become a part of the engineering practice.

The results of optical measurements provide valuable data for the simulation of complex physical processes, and are complementary to numerical simulation. Due to the complexity of the field, a systematic presentation and comparison of the different techniques is important, in order to support engineers with guidelines for solving a specific measurement problem.

ACKNOWLEDGMENTS

During the preparation of this manuscript, a great number of researchers showed their interest and support through stimulating discussions, and also kindly provided photographic material and illustrations for the publication. On this occasion, the authors would like to express their gratitude for these contributions.

8. REFERENCES

Auracher, H., Marroquin, A., 1989, A miniaturized sensor for local measurements in two-phase flow, to be presented at: 10th Brazilian Congress of Mechanical Engineering, Rio de Janeiro, Brasil.

Becker, H., Grigull, U., 1977, Interferometrie transparenter Phasenobjekte, insbesondere bei hohen Interferenzstreifendichten dargestellt an einem Beispiel aus der Wärmeübertragung, Wärme- und Stoffübertragung, Vol. 10, pp.233-244.

Brandt, A., Merzkirch, W., 1988, Measurement of droplet velocity in a spray jet by laser speckle velocimetry, 4 Int. Symp. on Applications of Laser Anemometry to Fluid Mechanics, Paper No. 1.14, Lisabon, Portugal.

Brüggeman, D., Hassel, E., Dittie, G., 1987, Single shot CARS measurements in a spark ignited engine, Joint meeting of the French and Italian sections of the combustion institute, Amalfi, Italy.

Chavez, A., 1990a, Impulsholografie, Beitrag I.4 für Hochschulkurs "Optische Methoden in der Wärme- und Stoffübertragung", Leiter F. Mayinger, Lehrstuhl A für Thermodynamik, TU München, FRG.

Chavez, A., 1990b, Rechnergestützte Auswertung von Hologrammen, Beitrag I.5 für Hochschulkurs "Optische Methoden in der Wärme- und Stoffübertragung", Leiter Prof. F. Mayinger, Lehrstuhl A für Thermodynamik, TU München, FRG.

Chavez, A., Mayinger, F., 1988, Evaluation of the pulsed laser holography for the characterization of sprays and direct measurements of drop size and velocity distributions, Proc. 1 World Congress Experimental Heat Transfer, Fluid Mechanics and Thermodynamics, Dubrovnik, Yugoslavia, pp. 848-855.

Chavez, A., Mayinger, F., 1989, Evaluation of pulsed laser holograms of spray droplets using digital image processing, prepared for: 2 Int. Congress on Paricle sizing, Tempe, Arizona, USA, 1990.

Chen, Yau-Ming, 1985, Wärmeübergang an der Phasengrenze kondensierender Blasen, Dissertation, Technical University of Munich, FRG.

Choudry, A., 1982, Automated digital processing of interferograms, Dissertation, Technical University of Delft, Holland.

Collier, R. J., Burckhardt, C. B., Lin, L. H., 1971, Optical holography, Academic Press, New York.

Dändliker, R., 1980, Heterodyne holographic interferometry, in Progress in Optics, Vol. XVII, North Holland, Amsterdam, pp. 1-84.

Durst, F., 1988, Optical techniques for fluid flow and heat transfer, Proc. 1 World Congress on Experimental Heat Transfer, Fluid Mechanics and Thermodynamics, Dubrovnik, Yugoslavia, pp. 32-47.

Durst, F., Melling, A., Whitelaw, J.H., 1987, Theorie und Praxis der Laser-Doppler-Anemometrie, G. Braun Verlag, Karlsruhe.

Emmerman, P.J., Goulard, R., Santoro, R.J., Semerjians, H.G., 1980, Multiangular absorption diagnostics of a turbulent argon-methane-jet, J. Energy, Vol. 4, p. 70.

Ennos, A. E., 1978, Speckle interferometry, in Progress in Optics, Vol. XVI, North Holland, Amsterdam, pp. 235-288.

Erbeck, R., 1985, Fast image processing with a microcomputer applied to speckle photography, Applied Optics, Vol. 24, No. 22, pp. 3838-3841.

Erbeck, R., 1986, Die Anwendung der Speckle Photographie zur statistischen Analyse turbulenter Dichtenfelder, VDI Verlag, Reihe 8, Nr. 112.

Erbeck, R., Merzkirch, W., 1988, Speckle photographic measurement of turbulence in an air stream with fluctuating temperature, Experiments in Fluids, Vol. 6, pp. 89-93.

Farrel, P. V., Hofeldt, D. L., 1984, Temperature measurement in gases using speckle photography, Applied Optics, Vol. 23, No. 7, pp.1055-1059.

Farrel, P. V., Springer, G. S., Vest, C. M., 1982, Heterodyne holographic interferometry, concentration and temperature measurements in gas mixtures, Applied Optics, Vol. 21, No. 9, pp. 1624-1627.

Farrel, P. V., Verhoeven, D. D., 1987, Heat transfer measurements in a motored engine using speckle interferometry, SAE Technical Paper Series, 870456, International Congress and Exposition, Detroit, Michigan, USA.

Friedrich, M., 1990, Dissipation in gerührten nicht-Newtonischen Flüssigkeiten, Dissertation, University of Hannover, FRG.

Gabor, D., 1948, A new microscopic principle, Nature, No. 161, pp. 777-778.

Gabor, D., 1949, Microscopy by reconstructed wavefronts, Proc. Roy. Soc. A 197, p. 454.

Gad-el-Hak, M., 1988, Visualization techniques for unsteady flows: an overview, ASME J. Fluids Eng., Vol. 110, pp. 231-243.

Gärtner, U., Wernekinck, U., Merzkirch, W., 1986, Velocity measurements in the field of an internal gravity wave by means of speckle photography, Experiments in Fluids, Vol.4, pp. 283-287.

Goldstein, R.J., Kreid, D.K., 1976, The laser-Doppler anemometer, in Measurements in Heat Transfer (Eckert, E.R.G., Goldstein, R.J., eds.), Hemisphere Publishing, McGraw-Hill, Washington, pp. 541-577.

Gross, K.P., McKenzie, R.L., Logan, P., 1987, Measurement of temperature, density, pressure, and their fluctuations in supersonic turbulence using laser-induced fluorescence, Experiments in Fluids, Vol. 5, pp. 372-380.

Guo, Z.-Y., Song, Y.-Z., Zhao, X.-W., 1988, Experimetal investigation on natural convection in channel by laser speckle photography, Proc. 1 World Congress Experimental Heat Transfer, Fluid Mechanics and Thermodynamics, Dubrovnik, Yugoslavia, pp. 412-418.

Haarde, W., 1989, Das Vermischen mit Hilfe von Flüssigkeitsstrahlen, Dissertation, University of Hannover, FRG.

Hariharan, P., 1984, Optical holography, Cambridge University Press.

Hariharan, P., Oreb, B. F., Brown, N., 1983, Real-time holographic interferometry: a microcomputer system for the measurement of vector displacements, Applied Optics, Vol. 22, No. 6, pp. 876-880.

Hassa, C., Paul, P.H., Hanson, R.K., 1987, Laser-induced fluorescence modulation techniques for velocity measurements in gas flows, Experiments in Fluids, Vol. 5, pp. 240-246.

Hauf, W., Grigull, U., 1970, Optical methods in heat transfer, in Advances in Heat Transfer, Vol. 6, Academic Press Inc., New York.

Herman, C. V., Mayinger, F., 1989, Experimental investigation of heat transfer in laminar forced convection flow in a grooved channel, prepared for: 9th Int. Heat Transfer Conf., Jerusalem, Israel.

Hesselink, L., 1989, Optical Tomography, In: Handbook of Flow visualization (ed. Yang, W. - J.), Hemisphere Publishing, Washington, pp. 307-329.

Hewitt, G.F., 1978, Measurement of two phase flow parameters, Academic Press, London.

Hewitt, G. F., 1987, Transient measurement techniques, ICHMT seminar: Transient phenomena in multiphase flow, Dubrovnik, Yugoslavia.

Hinsch, K., Mach D., Schipper W., 1983, Air flow analysis by double exposure speckle photography, Proc. 3 Int. Symp. Flow Visualization, Ann Arbor, Michigan, USA, pp. 576-580.

Howes, W. L., 1984, Rainbow schlieren and its applications, Applied Optics, Vol. 23, No. 14, pp. 2449-2460.

Hunter, J. C., Collins, M. W., 1987, Holographic interferometry and digital fringe processing, J. Phys. D: Appl. Phys. 20, pp. 683-691.

Hunter, J. C., Collins, M. W., 1989, Three-dimensional refractive index field reconstruction from holographic interferograms, Int. J. Optoelectronics, Vol. 4, No. 2, pp. 95-132.

Huntley, J. M., Palmer, S. J. P., Field, J. E., 1987, Automatic speckle photography fringe analysis: application to crack propagation and strength measurement, Proc. Int. Techn. Symp., San Diego, USA.

Inechen, B., Eglin, P., Dändliker, R., 1980, Hybrid optical and electronic image processing for strain measurements by speckle photography, Applied Optics, Vol. 19, No. 13, pp. 2191-2195.

Imaichi, K., Ohmi, K., 1983, Numerical processing of flow-visualization pictures — measurement of two-dimensional vortex flow, J. Fluid Mech., Vol. 129, pp. 283-311.

Jahn, M., 1975, Holographische Untersuchung der freien Konvektion in volumetrisch beheizten Fluiden, Dissertation, University of Hannover, FRG.

Janeschitz-Kriegel, H., 1983, Polymer melt rheology flow birefringence, Springer Verlag, Berlin.

Johnson, S. J., Fuller, G. G., 1986, Flowing colloidal suspensions in non-Newtonian suspending fluids: decoupling the composite birefringence, Rheol. Acta, Vol. 25, pp. 405-417.

Jones, R., Wykes, C., 1983, Holographic and speckle interferometry, A discussion of theory, practice and application of techniques, Cambridge University Press.

Kak, A. C., Slaney, M., 1988, Principles of computerized tomographic imaging, IEEE Press, New York.

Kawahashi, M., Toyooka, S., Hosoi, K., Suzuki, M., 1986, Speckle method for velocity masurement and visualization of flow, Proc. 4 Int. Symp. Flow Visualization, Paris, France, pp. 139-143.

Knauss, H., 1977, Ein Auswerteverfahren für allgemeine dreidimensionale Dichtefelder mit Hilfe der Interferenzmethode, Dissertation, University of Stuttgart, FRG.

Kreis, T., 1986, Auswertung holografischer Interferenzmuster mit Methoden der Ortsfrequenzanalyse, VDI Fortschritt-berichte, Reihe 8, Nr. 108.

Lauterborn, W., Vogel, A., 1984, Modern optical techniques in fluid mechanics, Ann. Rev. Fluid Mech., Vol. 16, pp.223-244.

Leipertz, A., 1981, Laser-Raman-Spektroskopie in der Wärme- und Strömungstechnik, Physik in unserer Zeit, Vol. 12, No. 4, pp. 107-115.

Leipertz, A., 1988, Messtechniken zur Untersuchung von Kohlenverbrennung in Flammen, BMFT-Status-Seminar "Verbrennungsforschung", 6 DVV-Kolloquium "Verbrennungeigenschaften von Kohlen", Essen, FRG.

Leipertz, A., 1989, Nutzung von Laser-Raman-Verfahren in der Verbrennungstechnik, Chem.-Ing.-Tech., Vol. 61, No. 1, pp. 39-48.

Leipertz, A., Knapp, K., 1984, Review on time-resolved two dimensional gas concentration mapping in turbulent flows using molecule sensitive light scattering techniques, Wärme- und Stoffübertragung, Vol. 18, pp. 237-245.

Liu, T. C., Merzkirch, W., Oberste-Lehn, K., 1989, Optical tomography applied to speckle photographic measurement of asymmetric flows with variable density, Experiments in Fluids,Vol. 7, pp. 157-163.

Lübbe, D., 1982, Ein Messverfahren für instationäre, dreidimensionale Verteilungen und seine Anwendungen auf Mischvorgänge, Dissertation, University of Hannover, FRG.

Mayinger, F., 1987, Modern noninvasive measuring techniques for transient two phase flow, ICHMT Seminar : Transient phenomena in multiphase flow, Dubrovnik, Yugoslavia.

Mayinger, F., Chen, Y. M., 1986, Heat transfer at the phase interface of condensing bubbles, Proc. 8 Int. Heat Transfer Conf., San Francisco, California, USA, pp. 1913-1918.

Mayinger, F., Lübbe, D., 1984, Ein tomographisches Meßverfahren und seine Anwendung auf Mischvorgänge und Stoffaustausch, Wärme- und Stoffübertragung, Vol. 18, pp. 49-59.

Mayinger, F., Panknin, W., 1974, Holography in heat and mass transfer, Proc. 5 Int. Heat Transfer Conf., Tokyo, Japan, pp. 28-43.

Merzkirch, W., 1987, Flow visualization, Academic Press, Orlando.

Mewes, D., Friedrich, M., Haarde, W., Ostendorf, W., 1989, Tomographic measurement techniques for process engineering studies, in Handbook of Heat and Mass Transfer, Gulf Publishing Company, Houston, Texas, Vol. 3, Chapter 24, pp. 951-1021.

Mewes, D., Ostendorf, W., 1983, Einsatz tomographischer Meßverfahren für verfahrenstechnische Untersuchungen, Chem.-Ing.-Tech., Vol.55, No.11, pp. 856-864.

Mewes, D., Renz, R., 1990, Grundlagen der Tomografie, Beitrag IV.1 für Hochschulkurs "Optische Methoden in der Wärme- und Stoffübertragung", Leiter F. Mayinger, Lehrstuhl A für Thermodynamik, TU München, FRG.

Mueller, T. J., 1980, On the historical development of apparatus and techniques for smoke visualization of subsonic and supersonic flows, AIAA Paper No. 80-0420-CP.

Nordmann, D., 1980, Temperatur, Druck und Wärmetransport in der Umgebung kondensierender Blasen, Dissertation, University of Hannover, FRG.

Osten, W., Saedler, J., Rottenkolber, H., 1987, Quantitative Auswertung von Interferogrammen mit einem digitalen Bildverarbeitungssystem, Technisches Messen, Vol.54, No.7/8, pp. 285-290.

Ostendorf, W., 1987, Einsatz der optischen Tomographie zum Messen von Temperaturfeldern in Rührgefässen, Dissertation, University of Hannover, FRG.

Ostendorf, W., Mayinger, F., Mewes, D., 1986, A tomographical method using holographic interferometry for the registration of three dimensional unsteady temperature profiles in laminar and turbulent flow, Proc. 8 Int. Heat Transfer Conf., San Francisco, California, USA, pp. 519-524.

Ostendorf, W., Mewes, D., 1988, Measurement of temperature fields in mixing vessels using optical tomography, Chem. Eng. Technol., Vol.11, pp. 148-155.

Ostrowski, Ju. I., 1988, Holografie - Grundlagen, Experimente und Anwendungen, Verlag Harri Deutsch, Thun.

Ostrovsky, Yu. I., Butusov, M. M., Ostrovskaya, G. V., 1980, Interferometry by holography, Springer-Verlag, Berlin.

Panknin, W., 1977, Eine holographische Zweiwellenlängen-Interferometrie zur Messung überlagerter Temperatur- und Konzentrationsgrenzschichten, Dissertation, University of Hannover, FRG.

Panknin, W., 1974, Einige Techniken und Anwendungen der holographischen Durchlichtsinterferometrie, CZ- Chemie- Technik, Sonderdruck 3, pp. 219 -225.

Penner, S. S., Jerskey, T., 1973, Use of lasers for local measurement of velocity components, species densities and temperatures, Ann. Rev. Fluid Mech., Vol. 5, pp. 9-30.

Philippoff, W., 1961, Elastic stresses and birefringence in flow, Trans. Soc. Rheology, Vol. 5, pp. 163-191.

Pindera, J. T., 1983, On theories and techniques of flow visualization using streaming birefringence: physical and phenomenological approaches, Proc. 3 Int. Symp. Flow Visualization, Ann Arbor, Michigan, USA, pp. 595-599.

Robinson, D., 1983, Automatic fringe analysis with a computer image processing system, Applied Optics, Vol. 22, No. 14, pp. 2169-2176.

Saffmann, M., 1989, Phasen-Doppler-Methode zur optischen Partikelgrößenmessung, Technisches Messen, Vol. 56, No. 7/8, pp. 298-303.

Santoro, R. J., Semerjian, H.G., Emmerman, P.J., Goulard, R., 1981, Optical tomography for flow field diagnostics, Int. J. Heat Mass Transfer, Vol. 24, No. 7, pp. 1139-1150.

Schardin, H., 1934, Das Toeplersche Schlierenverfahren, VDI Forschungsheft 367, Ausgabe B, Vol. 5.

Sernas, V., 1983, Interferometric methods in heat transfer research, Proc. 3 Int. Symp. Flow visualization, University of Michigan, Ann Arbor, Michigan, USA, pp. 753-762.

Settles, G. S., 1980, Color schlieren optics — a review of techniquies and applications, Proc. 2 Int. Symp. Flow visualization, Bochum, FRG.

Snyder, R., Hesselink, L., 1984, Optical tomography for flow visualization of the density field around revolving helicopter rotor blade, Applied Optics, Vol. 23, No. 20, pp. 3650-3656.

Snyder, R., Hesselink, L., 1985, High-speed optical tomography for flow visualization, Applied Optics, Vol. 24, No. 23, pp. 4046-4051.

Spindler, K., Bierer, M., Lorenz, G., Erhard, A., Hahne, E., 1988, Measurements in vertical gas liquid two-phase flows using an optical fiber probe, Proc. 1. World Congress Experimental Heat Transfer, Fluid Mechanics and Thermodynamics, Dubrovnik, Yugoslavia, pp. 348-357.

Stephan, M., Mayinger F., 1989, Countercurrent flow limitations in vertical ducts at high system pressures, to be presented at: 9th Int. Heat Transfer Conf., Jerusalem, Israel.

Stricker, W., 1988, Möglichkeiten und Grenzen der CARS-Messtechnik zur Temperaturbestimmung in Vebrennungssystemen, BMFT-Status-Seminar "Verbrennungsforschung", 6 DVV-Kolloquium "Verbrennungeigenschaften von Kohlen", Essen, FRG.

Strube, G. , 1990, Lineare Raman-Spektroskopie, Beitrag IV.2 für Hochschulkurs "Optische Methoden in der Wärme- und Stoffübertragung", Leiter F. Mayinger, Lehrstuhl A für Thermodynamik, TU München, FRG.

Uchiyama, H., Nakajima, M., Yuta, S., 1985, Measurement of flame temperature distribution by IR emission computed tomography, Applied Optics, Vol. 24, No. 23, pp. 4111-4116.

Van Dyke, M., 1982, An album of fluid motion, Parabolic Press, Stanford, California.

Verhoeven, D., Farrel, P. V., 1986, Speckle interferometry in transparent media, Applied Optics, Vol. 25, No. 6, pp. 903-906.

Vest, C. M., 1979, Holographic interferometry, John Wiley & Sons, New York.

Visualized flow, 1988, Compiled by the Japan Society of Mechanical Engineers, Pergamon Press, Oxford.

Walker, D.A., 1987, A fluorescence technique for measurement of concentration in mixing liquids, J. Phys. E. Sci. Instrum., Vol. 20., pp. 217-224.

Werle, H., 1973, Hydrodynamic flow visualization, Ann. Rev. Fluid Mech., Vol. 5, pp. 361-382.

Wernekinck, U., 1985, Anwendung der Speckle-Photographie zur Sichtbarmachung und Messung von Strömungen mit veränderlicher Dichte, VDI-Fortschritt-Berichte, Reihe 8, Nr. 95.

Wernekinck, U., Merzkirch, W., 1987, Speckle photography of spatially extended refractive index fields, Applied Optics, Vol.26, No.1, pp.31-32.

Wernike, G., Osten, W., 1982, Holografische Interferometrie, Physik Verlag, Weinheim.

Wiedemann, J., 1984, Laser-Doppler Anemometrie, Springer-Verlag, Berlin.

Willms, I., 1983, Anwendung computertomographischer Verfahren bei Aerosoldichtemessungen, Dissertation, University of Duisburg, FRG.

Winter, M., Lam, J.K., Long, M.B., 1987, Techniques for high-speed digital imaging of gas concentrations in turbulent flows, Experiments in Fluids, Vol. 5, pp. 177-183.

Wolfe, D.C., Byer, R.L., 1982, Model studies of laser absorption computed tomography for remote air pollution measurement, Applied Optics, Vol. 21, No. 7, pp. 1165-1178.

Zell, M., Straub, J., 1985, Experimentelle Untersuchung des Wärmeübergangs und seiner Transportmechanismen bei Siedevorgängen unter reduzierter Schwerkraft, Jahrbuch 1985 der Technischen Universität München, pp. 163-178.